

1 **Tyramine receptor drives olfactory response to (*E*)-2-decenal in the stink bug**  
2 ***Halyomorpha halys***

3

4 Luca Finetti<sup>1</sup>, Marco Pezzi<sup>1</sup>, Stefano Civolani<sup>1,2</sup>, Girolamo Calò<sup>3</sup>, Chiara Scapoli<sup>1</sup> and Giovanni  
5 Bernacchia<sup>1</sup>

6

7 <sup>1</sup>Department of Life Sciences and Biotechnology, University of Ferrara, Ferrara, Italy;

8 <sup>2</sup>InnovaRicerca s.r.l. Monestirolo, Ferrara, Italy; <sup>3</sup>Department of Biomedical and Specialty Surgical  
9 Sciences, Section of Pharmacology, University of Ferrara, Ferrara, Italy.

10

11 \*Author for correspondence: Giovanni Bernacchia, Department of Life Sciences and Biotechnology,  
12 University of Ferrara, via Luigi Borsari 46, Ferrara, Italy. Tel (+39) 0532 455784 [bhg@unife.it](mailto:bhg@unife.it)

13

14

15

16

17

18

19

20

21

22

23

24

25

26

27

28

29 **Abstract**

30 In insects, the tyramine receptor 1 (TAR1) has been shown to control several physiological functions,  
31 including olfaction. We investigated the molecular and functional profile of the *Halyomorpha halys*  
32 type 1 tyramine receptor gene (*HhTAR1*) and its role in olfactory functions of this pest. Molecular  
33 and pharmacological analyses confirmed that the *HhTAR1* gene codes for a true TAR1. The RT-  
34 qPCR analysis revealed that *HhTAR1* is expressed mostly in adult brain and antennae as well as in  
35 early development stages (eggs, 1<sup>st</sup> and 2<sup>nd</sup> instar nymphs). In particular, among the antennomeres  
36 that compose a typical *H. halys* antenna, *HhTAR1* was more expressed in flagellomeres. Scanning  
37 electron microscopy (SEM) investigation revealed the type and distribution of sensilla on adult *H.*  
38 *halys* antennae: both flagellomeres appear rich in trichoid and grooved sensilla, known to be  
39 associated with olfactory functions. Through a RNAi approach, topically delivered *HhTAR1* dsRNA  
40 induced a 50 % gene downregulation after 24 h in *H. halys* 2<sup>nd</sup> instar nymphs. An innovative  
41 behavioral assay revealed that *HhTAR1* RNAi-silenced 2<sup>nd</sup> instar nymphs were less susceptible to the  
42 alarm pheromone component (*E*)-2 decenal as compared to control. These results provide critical  
43 information concerning the TAR1 role in olfaction regulation, especially alarm pheromone reception,  
44 in *H. halys*. Furthermore, considering the emerging role of TAR1 as target of biopesticides, this work  
45 paves the way for further investigation on innovative methods for controlling *H. halys*.

46

47 **Keywords:** Brown Marmorated Stink Bug, TAR1 receptor, Antennae, Olfaction, Behavior, RNAi.

48

## 49 **Introduction**

50 Identifying volatile compounds through the olfactory system allows insects to find food sources,  
51 avoid predators as well as localize putative partners and oviposition habitats (Gadenne et al., 2016).  
52 Furthermore, the olfactory modulation by volatile molecules with repellent activity could be a  
53 promising strategy for pest control (Carey & Carlson, 2011). The basic organization of the olfactory  
54 system begins with the antennae, organs possessing cuticular structures, the sensilla, innervated by  
55 olfactory sensory neurons (OSNs) (Amin & Lin, 2019). The OSNs recognize different molecules  
56 through special olfactory receptors. Each OSN expresses only one type of olfactory receptor, ensuring  
57 the specificity of signal for a single odour (Zhao & McBride, 2020). When an OSN is activated, it  
58 sends the output signal through the axon to the antennal lobe. Here, excitatory projection neurons  
59 (PNs) transport the olfactory information to brain centres such as the mushroom body and the lateral  
60 horn (Tanaka et al., 2012). The mushroom body plays an important role in the olfactory learning and  
61 memory (Caron et al., 2013) while the lateral horn controls innate olfactory response functions  
62 (Jefferis et al., 2007). In insects, the olfactory system can be modulated by exogenous (photoperiod,  
63 temperature) and endogenous (hormones) factors.

64 The biogenic amines tyramine (TA) and octopamine (OA) are important neurohormones and  
65 neurotransmitters that play a key role in the regulation of primary mechanisms in invertebrates such  
66 as locomotion, learning memory and olfaction (Roeder, 2005). Initially, TA was considered only as  
67 a biosynthetic intermediate of OA (Lange, 2009), but later numerous studies showed that TA is indeed  
68 an important neurotransmitter (Blenau & Baumann, 2003; Roeder, 2005; Lange, 2009; Roeder, 2020).  
69 Among invertebrates, TA is the endogenous agonist of the tyramine receptors (TARs). Structurally,  
70 TARs receptors are part of the superfamily of G protein-coupled receptors sharing the typical  
71 structure with seven transmembrane domains (Ohta & Ozoe, 2014). Several studies have highlighted  
72 that TARs can be coupled with both  $G_q$  (increasing intracellular calcium levels) and  $G_i$  proteins  
73 (decreasing cAMP levels) (Saudou et al., 1990; Blenau et al., 2000; Enan, 2005; Rotte et al., 2009).  
74 Based on the rank order of potency of agonists, the TAR receptors have been classified into three  
75 different types (Wu et al., 2014): TAR1 and TAR2, coupled with  $G_q$  and  $G_i$  and proteins, while TAR3  
76 has been so far described only in *Drosophila melanogaster* (Bayliss et al., 2013; Wu et al., 2014).  
77 The first TAR1 was characterized in 1990 in *D. melanogaster* (Saudou et al., 1990). The receptor,  
78 called Tyr-dro, showed higher affinity (12-fold) for TA than for OA and was mainly expressed in  
79 heads. Since then the same receptor has been characterized in several orders of insects: Hymenoptera  
80 (Blenau et al., 2000), Orthoptera (Poels et al., 2001), Lepidoptera (Ohta et al., 2003), Hemiptera  
81 (Hana & Lange, 2017a) and Diptera (Finetti et al., 2020). Several physiological and behavioral  
82 functions are controlled by TAR1, including olfaction. In 2000 Kutsukake et al. characterized *honoka*,

83 a *D. melanogaster* strain that presented a TAR1 mutation and a compromised olfactory profile. These  
84 insects were not able to localize repellent stimuli suggesting that TAR1 could be involved in this  
85 physiological response. Furthermore, RNAi-mediated modulation of TAR1 expression was shown to  
86 affect the gregarious and solitary phase change through a different olfactory sensibility to attractive  
87 and repulsive volatiles (Ma et al., 2015). In honeybee antennae, an upregulation of TAR1 was  
88 observed during the transition from nurses to pollen foragers, suggesting a TAR1-regulation in their  
89 behavioral plasticity (McQuillan et al., 2012). High TAR1 levels were also found in the antennae of  
90 *Mamestra brassicae* and *Agrotis ipsilon*, further suggesting a pivotal role of this receptor in olfactory  
91 modulation (Brigaud et al., 2009; Dupontets et al., 2010). The TAR1s are considered interesting target  
92 for insecticides, especially bioinsecticides. Amitraz is an acaricide and non-systemic insecticide that  
93 targets the OA receptors. However, recent studies have shown that Amitraz can exert its toxic effect  
94 also through TAR1 activation (Wu et al., 2014; Kumar, 2019). Furthermore, a secondary metabolite  
95 of Amitraz, BTS-27271, increases the TA response on the *Rhipicephalus microplus* TAR1 (Gross et  
96 al., 2015). Concerning biopesticides, in the last years several studies have demonstrated that  
97 monoterpenes directly activate TAR1. In particular, Enan (2005) was the first to describe an agonist  
98 effect of several monoterpenes (thymol, carvacrol,  $\alpha$ -terpineol, eugenol) on the *D. melanogaster*  
99 TAR1. However, the same monoterpenes did not show the same pharmacological profile on *D.*  
100 *suzukii* and *R. microplus* TAR1 receptors where they act as positive allosteric modulators (Gross et  
101 al., 2017; Finetti et al., 2020).

102 *H. halys* (Rhyncota; Pentatomidae) is an insect typical of the Eastern Asia (China, Japan, Taiwan,  
103 and Korea) (Haye et al., 2015), was detected for the first time in USA in 1998 (Hoebeke & Carter,  
104 2003) and became a stable presence in orchards since 2010 (Rice et al., 2014). Its first European  
105 appearance was reported in 2004 in Switzerland then leading to its spread across the continent (Cesari  
106 et al., 2018). *H. halys* is responsible for major damages to many economically relevant crops (Leskey  
107 & Nielsen, 2018). The damages are caused by the perforation of the external integuments of fruits by  
108 the rostrum, the specialized sucking apparatus typical of Rhynchota. This causes necrotic areas on  
109 fruits, as well as the transmission of other phytopathogens, leading to a relevant devaluation of the  
110 product (Peiffer & Felton, 2014). In the Asiatic regions, the life cycle of *H. halys* consists of only one  
111 generation per year (Lee et al., 2013). However, in warmer regions, the insect is able to complete up  
112 to four annual generations, significantly increasing its number in the area (each female is able to lay  
113 between 100 and 500 eggs for cycle) (Nielsen et al., 2016). This particular phytopathogen shows high  
114 resistance to common pesticides, making difficult its control and elimination (Bergmann & Raupp,  
115 2014).

116 The present work describes the role of TAR1 in *H. halys* olfaction. Through a RNAi-mediated  
117 knockdown of *HhTAR1* expression, the olfaction response to the alarm pheromone component (*E*-  
118 2-decenal was studied with an innovative behavioral assay. These findings shed light on the  
119 importance of the TAR1 receptor in *H. halys* and might contribute to develop new control tools  
120 against this pest.

121

## 122 **Materials and Methods**

### 123 **Insects and Reagents**

124 Individuals of *H. halys* were reared on green beans and kiwi with a photoperiod of 16 h light: 8 h  
125 dark, at a temperature of  $24 \pm 1$  °C. Tyramine hydrochloride, octopamine hydrochloride, yohimbine  
126 hydrochloride,  $\gamma$ -aminobutyric acid, serotonin hydrochloride, epinephrine, norepinephrine, brilliant  
127 black, Bovine Serum Albumin (BSA), probenecid, 4-(2-hydroxyethyl)-1-piperazineethanesulfonic  
128 acid (HEPES), (*E*)-2-decenal were all obtained from Sigma-Aldrich (St. Louis, Missouri, USA).  
129 Dopamine was obtained from Tocris Bioscience (Bristol, United Kingdom). Pluronic acid and  
130 fluorescent dye Fluo-4 AM were purchased from Thermo Fisher Scientific (Waltham, Massachusetts,  
131 USA). All compounds were dissolved in dimethyl sulfoxide (10 mM) and stock solutions were kept  
132 at -20 °C until use. Serial solutions were made in the assay buffer (Hanks' Balanced Salt solution  
133 (HBSS)/HEPES 20 mM buffer, containing 0.01 % BSA and 0.1 % DMSO).

134

### 135 **Isolation and cloning of full-length HhTAR1**

136 Total RNA was extracted from four adults of *H. Halys* using RNAgent® Denaturing Solution  
137 (Promega, Madison, Wisconsin, USA), quantified in a micro-volume spectrophotometer Biospec-  
138 Nano (Shimadzu, Kyoto Japan) and analysed by 0.8 % w/v agarose gel electrophoresis. One  $\mu$ g of  
139 RNA was treated with DNase I (Thermo Fisher Scientific) and used for the synthesis of cDNA,  
140 carried out with the OneScript® Plus cDNA Synthesis Kit (ABM, Richmond, Canada). For  
141 amplification of the full *HhTAR1* open reading frame (ORF), specific primers were designed based  
142 on the annotated transcript (XM\_014422850.2). The Kozak translation initiation sequence  
143 (GCCACC) was inserted at 5' end of the receptor (**Table 1**). High fidelity amplification was achieved  
144 using Herculase II Fusion DNA Polymerase (Agilent, Santa Clara, California, USA) and a touchdown  
145 thermal profile: predenaturation at 95 °C for 3 mins, followed by 10 cycles at 95 °C for 20 s, 65-55  
146 °C for 20 s (minus 1 °C/cycle), 68 °C for 2 mins, 30 cycles at 95 °C for 20 s, 55 °C for 20 s, 68 °C  
147 for 2 mins and a final extension at 68 °C for 4 mins. The PCR product was gel purified by Illustra  
148 GFX PCR DNA and Gel Band Purification Kits (GE Healthcare, Chicago, Illinois, USA), cloned into  
149 pJET 1.2/blunt vector (Thermo Fisher Scientific) and transformed into *E.coli* SIG10 5- $\alpha$  Chemically

150 Competent Cells (Sigma-Aldrich). Positive clones were selected using LB broth agar plates with 100  
151  $\mu\text{g/ml}$  ampicillin. Plasmid was then extracted by GenElute™ Plasmid Miniprep Kit (Sigma-Aldrich)  
152 and verified by DNA sequencing (BMR Genomics, Padua, Italy). The sequence, named *HhTAR1*,  
153 was deposited in GenBank with the accession number MT513133. For expression in Human  
154 Embryonic Kidney (HEK 293) cells, the open reading frame of *HhTAR1* was excised from pJET 1.2  
155 vector and inserted into the pcDNA 3.1 (+) Hygro expression vector using *Xho I* and *Xba I* restriction  
156 sites.

157

### 158 **Multiple sequence alignment and general bioinformatics analysis**

159 Multiple protein sequence alignments between the deduced amino acid sequence of HhTAR1 and  
160 other type 1 tyramine receptor sequences were performed using Clustal Omega  
161 (<https://www.ebi.ac.uk/Tools/msa/clustalo/>) and BioEdit Sequence Alignment Editor 7.2.6.1.  
162 Phylogenetic neighbour-joining analysis was performed by MEGA software (version 7) with 1000-  
163 fold bootstrap resampling. The *D. melanogaster* GABA B receptor (GABABR) was used as an  
164 outgroup to root the tree.

165

### 166 **HhTAR1 transient expression in HEK 293**

167 HEK 293 cells were grown at 37 °C and 5 % CO<sub>2</sub> in Dulbecco's modified Eagles medium high  
168 glucose (D-MEM) supplemented with 10 % fetal bovine serum (Euroclone, Milan, Italy). To prevent  
169 bacterial contamination, penicillin (100 U/ml) and streptomycin (0.1 mg/ml) were added to the  
170 medium. The cells were transiently transfected with pcDNA 3.1 (+) / HhTAR1 in T75 cell culture  
171 flasks (Euroclone) using JetOPTIMUS (Polyplus-Transfection, New York, New York, USA),  
172 following the manufacturer's protocol. Cells were incubated in the transfection medium for 24 h at  
173 normal cell growth conditions before their use for the calcium mobilization assay.

174

### 175 **Calcium Mobilization Assay**

176 Cells were seeded at a density of 50,000 cells per well, total volume of 100  $\mu\text{l}$ , into poly-D- lysine  
177 coated 96-well black, clear-bottom plates. After 24 h incubation at normal cell culture condition, the  
178 cells were incubated with HBSS 1X supplemented with 2.5 mM probenecid, 3  $\mu\text{M}$  of the calcium  
179 sensitive fluorescent dye Fluo-4 AM and 0.01 % pluronic acid, for 30 mins at 37 °C. After that, the  
180 loading solution was removed and HBSS 1X supplemented with 20 mM HEPES, 2.5 mM probenecid  
181 and 500  $\mu\text{M}$  brilliant black were added. Cell culture and drug plates were placed into the fluorometric  
182 imaging plate reader FlexStation II (Molecular Devices, Sunnyvale, California, USA) and  
183 fluorescence changes were measured after 10 mins of stabilization at 37 °C. On-line additions were

184 carried out in a volume of 50  $\mu$ l/well after 20 s of basal fluorescence monitoring. In antagonism  
185 protocols, to facilitate drug diffusion into the wells the assays were performed at 37 °C with three  
186 cycles of mixing (25  $\mu$ l from each well moved up and down three times). The fluorescence readings  
187 were measured every two s for 120 s.

188

### 189 **Quantitative real-time PCR analysis**

190 Total RNA was extracted from *H. halys* samples at various developmental stages (eggs, 1<sup>st</sup> to 5<sup>th</sup>  
191 instar nymphs, adult males and females) and different organs (antennae, brain, midgut, reproductive  
192 organs) using RNAgent® Denaturing Solution (Promega). The organs of *H. halys* were dissected in  
193 a RNA preservation medium (20 mM EDTA disodium (pH 8.0), 25 mM sodium citrate, 700 g/l  
194 ammonium sulphate, final pH 5.2). One  $\mu$ g of purified RNA was then treated with DNase I (Thermo  
195 Fisher Scientific) and used for cDNA synthesis, carried out with OneScript® Plus cDNA Synthesis  
196 Kit (ABM), according to the manufacturer's instructions. Real time PCR was performed using a CFX  
197 Connect Real-Time PCR Detection System (Bio-Rad) in a 12  $\mu$ l reaction mixture containing 0.8  $\mu$ l  
198 of the cDNA obtained from 1  $\mu$ g of total RNA, 6  $\mu$ l ChamQ SYBR qPCR Master Mix (Vazyme,  
199 Nanchino, China), 0.4  $\mu$ l forward primer (10  $\mu$ M), 0.4  $\mu$ l reverse primer (10  $\mu$ M) and 3.6  $\mu$ l nuclease  
200 free water. Thermal cycling conditions were: 95 °C for 2 mins, 40 cycles at 95 °C for 15 s and 60 °C  
201 for 20 s. After the cycling protocol, a melting-curve analysis from 60 °C to 95 °C was applied.  
202 Expression of *HhTARI* was normalized in accordance with the relative quantitation method (Larionov  
203 et al., 2005) using *ARP8* and *UBE4A* as reference genes (Bansal et al., 2016). Gene-specific primers  
204 (**Table 1**) were used and at least three independent biological replicates, made in triplicate, were  
205 performed for each sample.

206

### 207 **Antennae preparation and SEM analysis**

208 Preliminary morphological investigations were performed on ten adults of *H. halys* (five males and  
209 five females) using a Nikon SMZ 800 stereomicroscope (Nikon Instruments Europe, Amsterdam,  
210 The Netherlands), provided with a Nikon Digital Sight Ds-Fil camera (Nikon Instruments Europe,  
211 Amsterdam, The Netherlands) and connected to a personal computer with the imaging software NIS  
212 Elements Documentation (Nikon Instruments Europe, Amsterdam, The Netherlands). Based on  
213 stereomicroscope observations, the head was dissected from body and prepared for scanning electron  
214 microscopy (SEM), according to previously published procedures (Pezzi et al. 2015, 2016).  
215 Afterwards, samples were critical point dried in a Balzers CPD 030 dryer (Leica Microsystems,  
216 Wetzlar, Germany), glued on stubs and coated with gold-palladium in an S150 Edwards sputter coater

217 (HHV Ltd, Crawley, United Kingdom). The SEM observations were conducted at the Electronic  
218 Microscopy Centre of the University of Ferrara, using a Zeiss EVO 40 SEM (Zeiss, Milan, Italy).

219

## 220 **Synthesis of dsRNA and *H. halys* treatment**

221 For RNAi silencing, *HhTAR1* and *LacZ* (control) amplicons, 400-500 bp long, were generated by  
222 PCR using primers with 5' extensions containing T7 promoters (**Table 1**). These products were  
223 cloned into pJET 1.2 vector (Thermo Fisher Scientific) and then used as templates for *in vitro* dsRNA  
224 synthesis performed by T7 RNA Polymerase (Jena Bioscience, Jena, Germany), according to the  
225 manufacturer's protocol. After one hour of synthesis at 37 °C, a DNase I (Thermo Fisher Scientific)  
226 treatment was performed and the dsRNA was clean up by ammonium acetate precipitation (Rouhana  
227 et al., 2013). Finally, the dsRNA was resuspended in ultrapure water and quantified by Biospec-Nano  
228 spectrophotometer. To induce RNAi silencing 2<sup>nd</sup> stage nymphs of *H. halys* 3 days post-ecdysis were  
229 treated with 100 ng of dsTAR1 or dsLacZ in 1 µl of solution using a 0.1-2 µl micropipette. The  
230 dsRNA molecules were topically delivered through a drop placed on the abdomen of nymphs  
231 (**Supplementary figure 4**). Insects were tested by behavioral assay after 24 h while the *HhTAR1*  
232 transcript level was measured by RT-qPCR, as described above.

233

## 234 **Repellence assay**

235 An open petri dish (90 mm x 15 mm), containing 24 h starved *H. halys* 2<sup>nd</sup> instar nymphs and a green  
236 bean, was placed inside a plexiglas box (50 cm each side) with two lateral openings covered by nets  
237 to allow air circulation. The negative control acetone or the positive repellent control (*E*)-2-decenal  
238 were applied to a filter paper (1 cm x 1 cm) that was placed under the green bean. The positive control  
239 (*E*)-2-decenal, dissolved in acetone, was tested at a fixed quantity of 10 µg, a value ensuring the  
240 maximum repellence activity against the *H. halys* nymphs (Zhong et al., 2018). The number of *H.*  
241 *halys* nymphs standing and feeding on the green bean was monitored every ten minutes for one hour.  
242 Four biological replicates were made, each comprising at least ten insects, for both untreated and  
243 dsRNA treated *H. halys* nymphs. All experiments were performed in the morning in a behavioral  
244 room with a controlled temperature of 24 ± 1 °C.

245

## 246 **Data analysis and terminology**

247 All data were elaborated using Graph Pad Prism 6.0 (La Jolla, California, USA). Data are expressed  
248 as mean ± SEM of n experiments and were analysed using one- or two-way analysis of variance  
249 (ANOVA) followed by Dunnett's or Turkey's test for multiple comparison. In the pharmacological  
250 assays, the concentration-response curves were fitted using the four parameters log logistic equation:



251 
$$\text{Effect} = \text{Baseline} + \frac{(\text{E}_{\text{max}} - \text{Baseline})}{(1 + 10^{(\text{LogEC}_{50} - \text{Log}[\text{compound}]) * \text{Hillslope}})}$$

252 Agonist potency was expressed as pEC<sub>50</sub>, defined as the negative logarithm to base 10 of the agonist  
253 molar concentration that produces 50% of the maximum possible effect of that agonist. Antagonist  
254 potency was derived from Gaddum Schild equation:

255 
$$\text{pA}_2 = -\log \left[ \frac{\text{CR} - 1}{\text{antagonist}} \right]$$

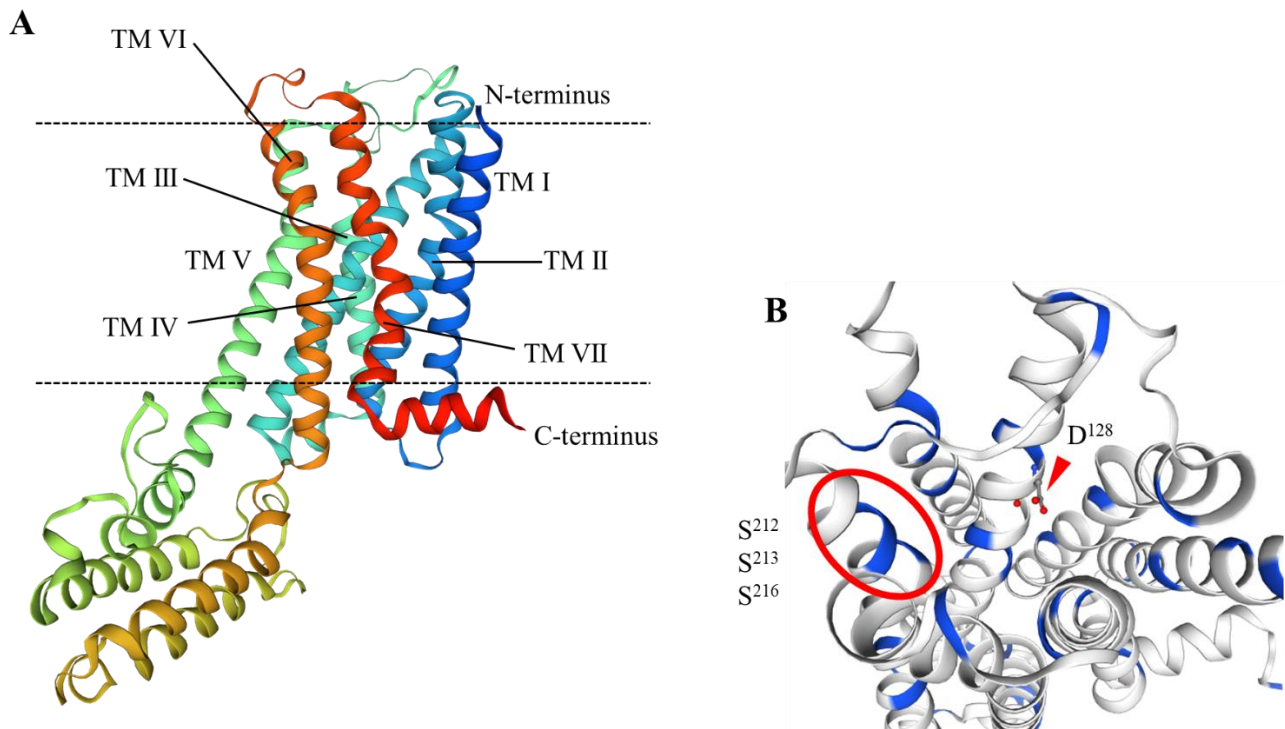
256 Assuming a slope value equal to unity, where CR indicates the ratio between agonist potency in the  
257 presence and absence of antagonist (Kenakin, 2014).

258

## 259 **Results**

### 260 **Molecular characterization of HhTAR1**

261 The amplified *HhTAR1* sequence was 1347 bp long and coded for a 449 aa polypeptide with a  
262 predicted MW of 50.97 KDa and pI of 9.41. About structural domains, both TMHMM v 2.0 software  
263 and the Kyte and Doolittle method (Kyte & Doolittle, 1982) suggest seven putative transmembrane  
264 domains, as expected for a GPCR. The helices are flanked by an extracellular N-terminus of 51  
265 residues and an intracellular C-terminus of 18 residues. Furthermore, the HhTAR1 sequence contains  
266 a DRY conserved sequence in the TM3, several N-glycosylation sites in the extracellular N-terminus  
267 and P-glycosylation sites, 2 specific for PKA and 10 specific for PKC (**Supplementary Figure 1**).  
268 These features are important for the correct folding and function of GPCRs (Nørskov-Lauritsen &  
269 Bräuner-Osborne, 2015). Moreover, at position 128 in TM3 there is a conserved aspartic acid (D<sup>128</sup>,  
270 shown in **Figure 1, panels A and B**) responsible for the interaction with TA, the endogenous agonist  
271 of the TAR1s (Ohta & Ozoe, 2014).



272

273 **Figure 1.** Structural overview of HhTAR1 predicted by SWISS-MODEL. **(A)** Model of the whole receptor showing the  
274 transmembrane domains. **(B)** Detail of the putative ligand binding pocket, seen from the extracellular side, of HhTAR1.  
275 All serine residues are highlighted in blue. The aspartic acid in TM3 (D<sup>128</sup>) is shown by a triangle and the three serine  
276 residues interacting with TA are highlighted by a circle.  
277

278 To study the binding site structure, the HhTAR1 aminoacidic sequence was analysed by SWISS-  
279 MODEL (Waterhouse et al., 2018). The model was created based on the crystal structure of the human  
280  $\alpha$ 2A adrenergic receptor (Template code: 6kux.1.A) that shares 33.51 % of sequence identity with  
281 HhTAR1. The three-dimensional model of the whole receptor and the putative ligand binding pocket  
282 are shown in **Figure 1**. In 2004, several serine residues in TM V were found to play a key role in  
283 stabilizing the interaction with TA in *Bombyx mori* and *Sitophilus oryzae* (Ohta et al., 2004; Braza et  
284 al., 2019) TAR1. These serine residues localized in the TM V are also conserved in HhTAR1 at  
285 positions S<sup>212</sup>, S<sup>213</sup> and S<sup>216</sup> (**Figure 1, panel B**). MolProbity model quality investigation (**Table 2**)  
286 confirmed the validity of the SWISS-MODEL 3D model of HhTAR1 (Chenn et al., 2010). The  
287 HhTAR1 deduced amino acid sequence was then compared to several OA and TA receptors allowing  
288 the construction of a neighbour-joining phylogenetic tree by MEGA 7 server (**Supplementary**  
289 **Figure 2**). As expected, HhTAR1 grouped in the TAR1 family, the main monophyletic group, and  
290 shared the highest percentage of identity with the *Rhodnius prolixus* TAR1 (Accession number:  
291 MF377527.1), another Pentatomidae. Based on the phylogenetic results, a multiple sequence  
292 alignment was performed between the HhTAR1 deduced amino acid sequence and TAR1 from other  
293 insects (**Figure 2**). The analysis further strengthen the similarity of HhTAR1 with known TAR1

294 receptors showing the typical GPCR structure with highly conserved domains corresponding to the  
 295 transmembrane regions as well as the TA binding site.

296



297

298

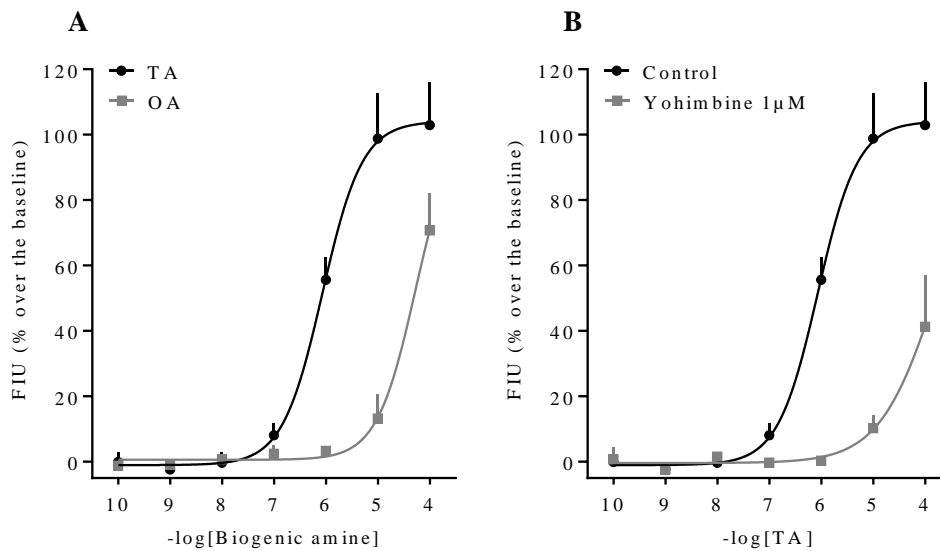
299 **Figure 2.** Amino acid sequence alignment of HhTAR1 with orthologous receptors from  
 300 *R. prolixus* (RpTAR1), *D. melanogaster* (DmTAR1) *Phormia regina* (PrTAR1), *Mamestra brassicae* (MbTAR1), *Chilo*  
 301 *suppressalis* (CsTAR1) and *Rhipicephalus microplus* (RmTAR1). The putative seven transmembrane domains (TM I-  
 302 VII) are indicated with a black line. Identical residues are highlighted in black while conservative substitutions are shaded  
 303 in grey. A red triangle indicates the conserved aspartic acid D<sup>128</sup> and the serine residues that could interact with TA are  
 304 shown by a red box.

305

### 306 HhTAR1: pharmacological validation

307 In the calcium mobilization assay HhTAR1 was activated by both TA and OA in a concentration-  
 308 dependent manner (**Figure 3, panel A**). TA evoked the release of intracellular calcium with pEC<sub>50</sub>  
 309 values of 5.99 (CL<sub>95%</sub> 5.32-6.66) and E<sub>max</sub> of 109.33 ± 14.86, while OA resulted less potent with a  
 310 pEC<sub>50</sub> of 4.41 (4.17-4.64) calculated assuming the TA maximum effect (**Figure 3, panel A**). In wild  
 311 type HEK 293 cells, TA and OA were completely inactive when tested in the same concentration  
 312 range (from 10<sup>-10</sup> M to 10<sup>-4</sup> M) (data not shown). Yohimbine was completely inactive as agonist,

313 while, at 1  $\mu\text{M}$  yohimbine, elicited a rightward shift of the concentration response curve to TA  
314 (**Figure 3, panel B**); a  $pA_2$  of 8.26 was calculated from these experiments.



315  
316 **Figure 3.** Calcium mobilization assay in HhTAR1-transfected HEK293 cells. Concentration-response curves to TA and  
317 OA (A). Concentration-response curves to TA in the absence (control) and in presence of 1  $\mu\text{M}$  yohimbine (B). Data are  
318 means  $\pm$  SEM of three separate experiments performed in duplicate.  
319

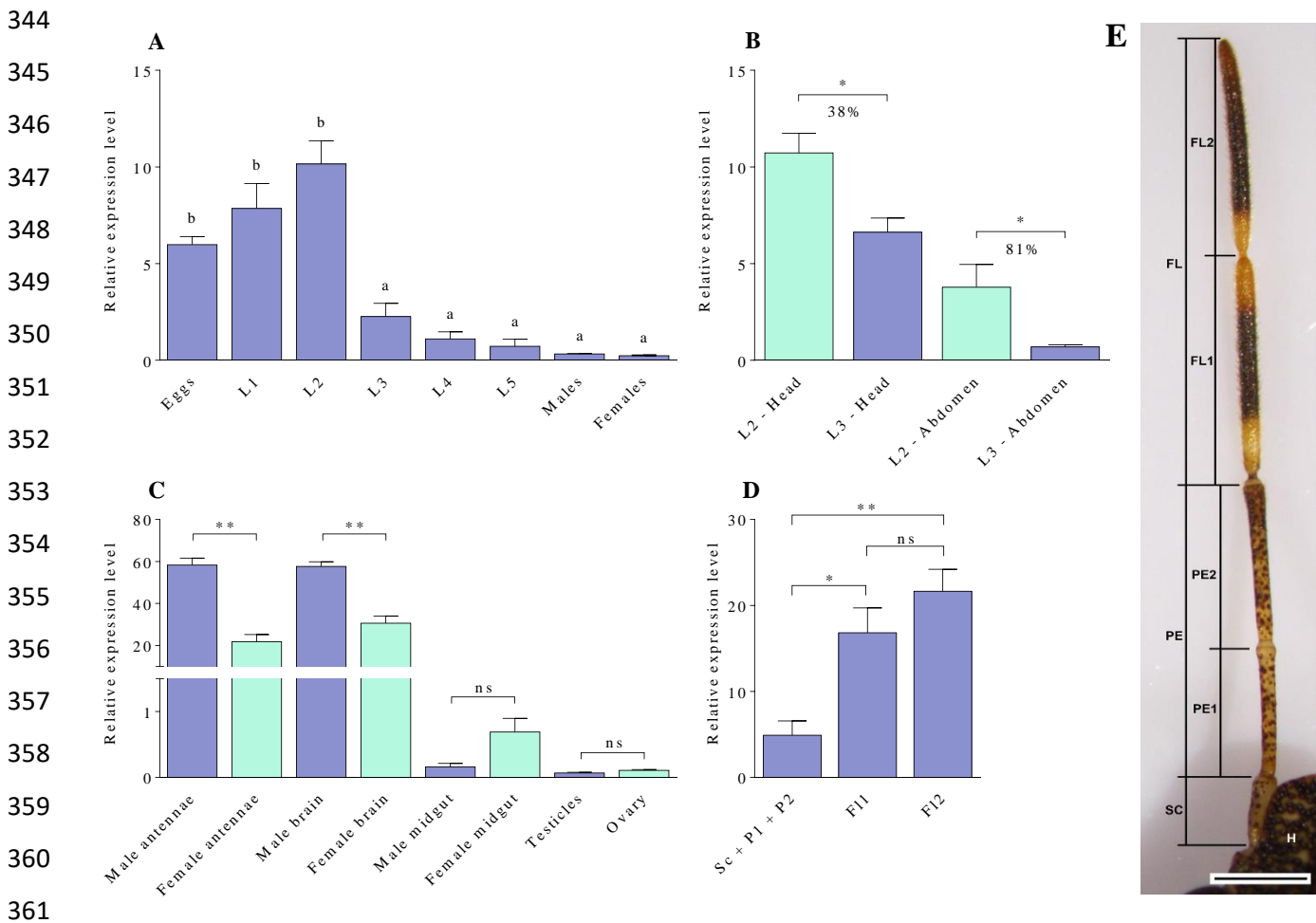
320 In order to confirm the HhTAR1 sensibility to TA and OA, other biogenic amines such as dopamine,  
321 L-DOPA, epinephrine, norepinephrine and serotonin or important neurotransmitter like  $\gamma$ -  
322 aminobutyric acid were tested at  $10^{-4}$  M as putative ligands. TA and OA were able to generate a potent  
323 effect against the receptor while the other molecules did not elicit any release of calcium  
324 (**Supplementary Figure 3**).

325

### 326 *HhTAR1* expression pattern

327 Given the importance of TAR1s in insect physiology and behavior, *HhTAR1* expression profile was  
328 studied in all *H. halys* development stages (egg, 1<sup>st</sup> to 5<sup>th</sup> instar nymphs, L1 to L5, and adult) as well  
329 as in the major organs of the adult. The analysis revealed that *HhTAR1* was mostly expressed in eggs  
330 and in 1<sup>st</sup> and 2<sup>nd</sup> instar nymphs, with a dramatic decrease in receptor mRNA levels in the later stages  
331 from the 3<sup>rd</sup> instar nymph to adult (**Figure 4, panel A**). This mRNA reduction in 2<sup>nd</sup> and 3<sup>rd</sup> instar  
332 nymphs was further investigated. The nymphs were divided in two parts: head + antennae and thorax  
333 + abdomen and the *HhTAR1* expression levels analysed. The *HhTAR1* mRNA level decrease affected  
334 both sections of 2<sup>nd</sup> and 3<sup>rd</sup> instar nymphs with different intensity (**Figure 4, panel B**): the level in  
335 head/antennae decreased only by 38% between L2/L3, while it dropped by 82 % in thorax/abdomen.  
336 This reveals that *HhTAR1* levels remain high in the nervous tissues while they decrease significantly  
337 in the rest of the nymph body. Among the different organs analysed (antennae, brains, midguts and

338 gonads), the highest levels of *HhTAR1* transcript were detected in the brains and the antennae of both  
 339 sexes, even if they were statistically more abundant in male tissues (**Figure 4, panel C**). Furthermore,  
 340 *HhTAR1* expression was investigated in all antennomeres of *H. halys*. The antenna is in fact composed  
 341 by a scape (SC), two pedicels (PE1 and PE2) and two flagellomeres (FL1 and FL2) (**Figure 4, panel**  
 342 **E**). The *HhTAR1* mRNA was detected in all antennomeres but it was 2-3 times more abundant in FL1  
 343 and FL2 in comparison to SC and both elements of pedicel (**Figure 4, panel D**).



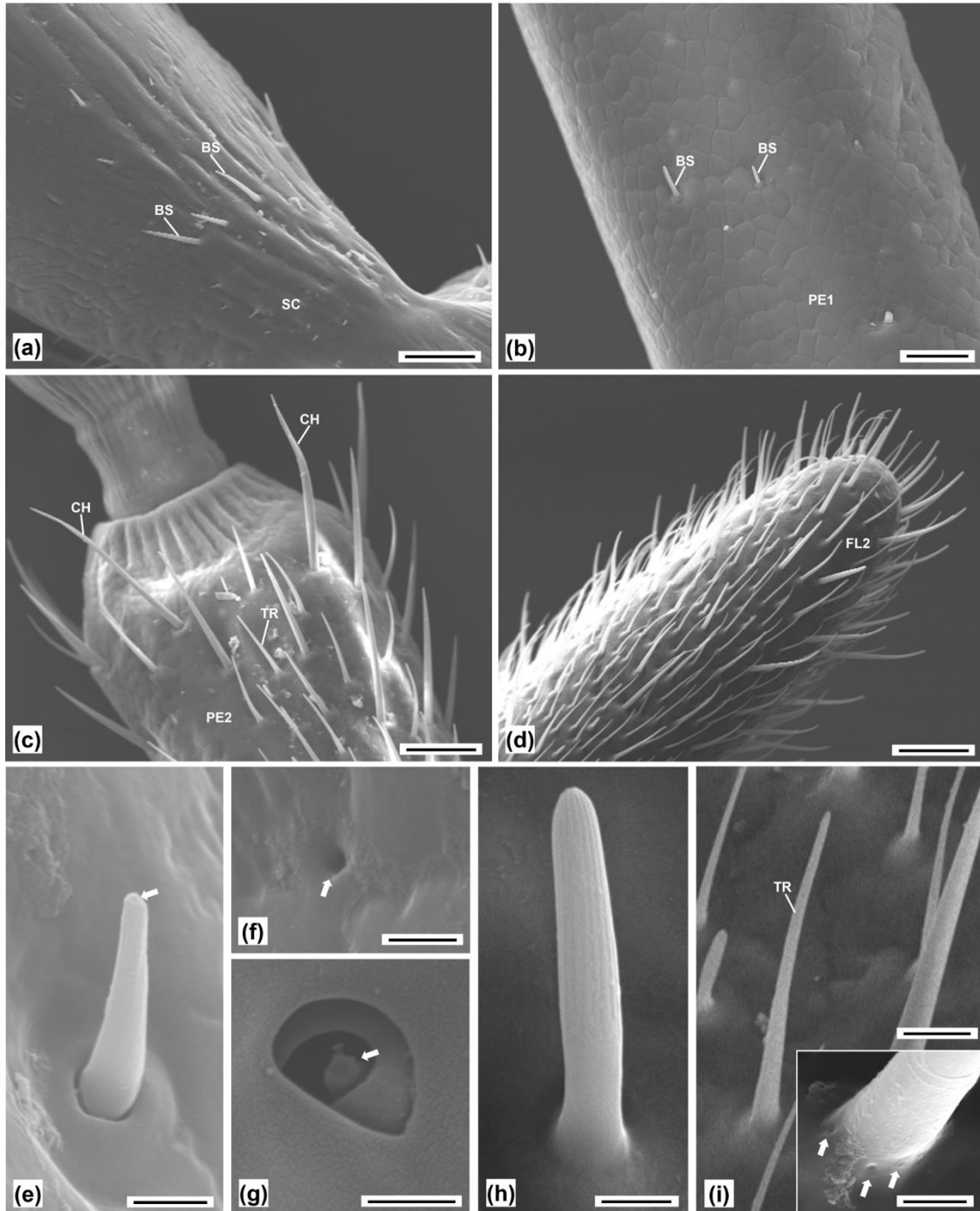
362 **Figure 4.** mRNA expression levels of *HhTAR1* gene. **(A)** Expression of *HhTAR1* gene in all development stages: eggs,  
 363 1<sup>st</sup> to 5<sup>th</sup> instar nymphs (L1 to L5), adult male and female. **(B)** Expression of *HhTAR1* in different parts of 2<sup>nd</sup> (L2) and  
 364 3<sup>rd</sup> (L3) *H. halys* instar nymphs. **(C)** Expression of *HhTAR1* gene in organs of both sexes. **(D)** Expression of *HhTAR1* in  
 365 different parts of adult *H. halys* antennae. Data represent means  $\pm$  SEM of at least three independent experiments  
 366 performed in triplicate. \*  $p < 0.05$  \*\*  $p < 0.01$  according to one-way ANOVA followed by multiple comparisons  
 367 Bonferroni post-hoc. **(E)** Antenna structure of the adult *H. halys* observed on a stereomicroscope. FL, flagellum; FL1,  
 368 first segment of flagellum; FL2, second segment of flagellum; H, head; PE, pedicel; PE1, first segment of pedicel; PE2,  
 369 second segment of pedicel; SC, scape.

370

### 371 Sensilla investigation by SEM

372 The different expression of *HhTAR1* in antennomeres required a further characterization of the  
 373 antenna. The antennae, the main organs of the olfactory system in insects, are rich in sensilla whose  
 374 morphology correlates with their physiological role. We investigated by scanning electron  
 375 microscopy (SEM) the morphology and distribution of sensilla in the different parts of adult *H. halys*

376 antennae: scape (SC), two pedicels (PE1 and PE2) and two flagellomeres (FL1 and FL2) (**Figure 4,**  
377 **panel E**). In the SC and both PEs, sporadic basiconic sensilla (BS) (**Figure 5, panels A, B and E**)  
378 were visible along with particular perforations classified as pit sensilla (PT), or coeloconic sensilla,  
379 found in both PEs (**Figure 5, panels F and G**). Several chaetic sensilla (CH) were observed in the  
380 PE2-FL1 junction area (**Figure 5, panel C**). A high number of sensilla was found in both FLs,  
381 classified as trichoid (TR) (**Figure 5, panels D and I**), basiconic (BS), or grooved sensilla (**Figure**  
382 **5, panel H**).

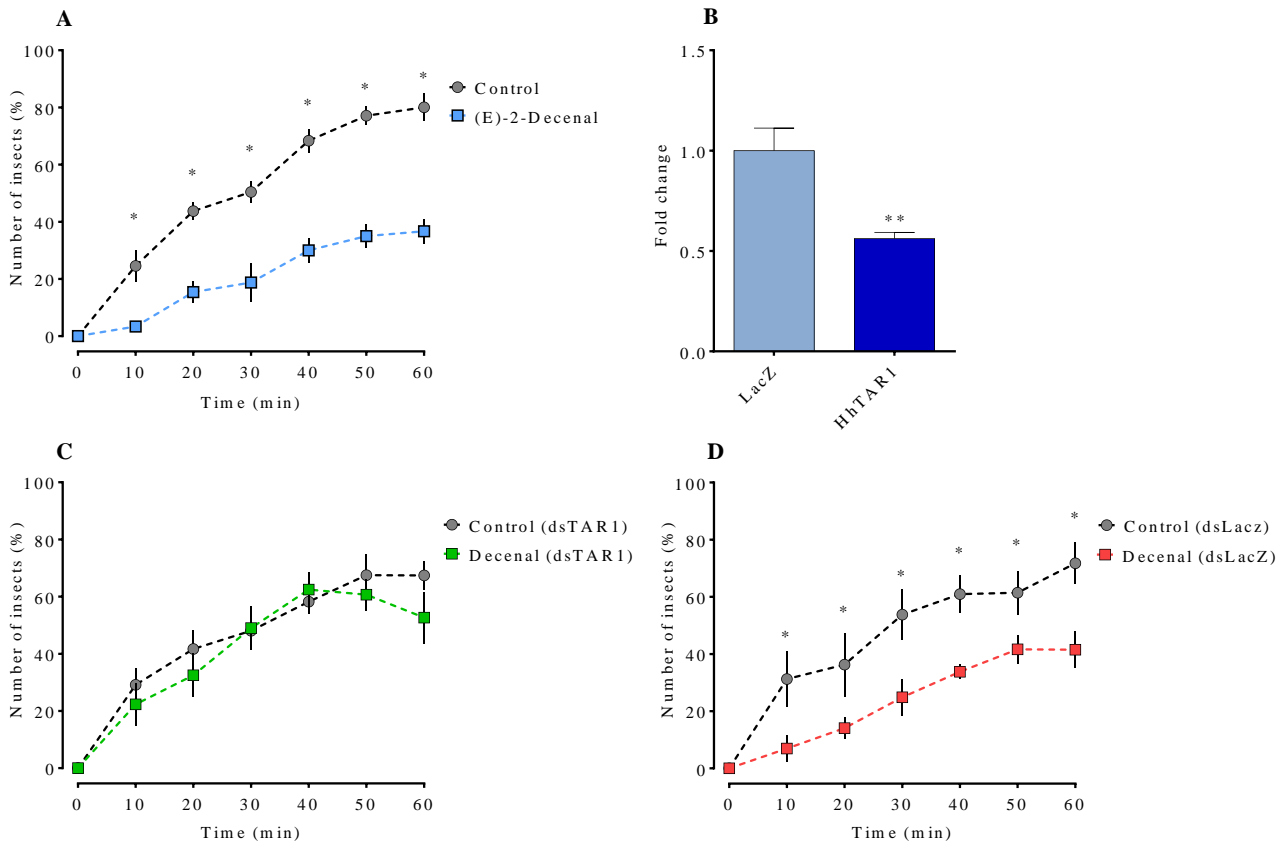


383  
384 **Figure 5.** Antennae of adult *H. halys* observed at the scanning electron microscope (SEM) (**A-I**). (**A**) Female antenna,  
385 detail of the base of the scape. Scale bar 50µm. (**B**) Male antenna, detail of the first segment of the pedicel base of the  
386 scape. Scale bar 25µm. (**C**) Male antenna, distal part of the second segment of the pedicel. Scale bar 50µm. (**D**) Male

387 antenna, tip of the second segment of the flagellum. Scale bar 50 $\mu$ m. (E) Female antenna, basiconic sensillum of the scape  
388 with a tip perforation (arrow). Scale bar 2.5 $\mu$ m. (F) Male antenna, perforation of the pedicel (arrow). Scale bar 1.5 $\mu$ m.  
389 (G) Female antenna, pit sensillum of the pedicel, containing a peg (arrow). Scale bar 1.5 $\mu$ m. (H) Female antenna, grooved  
390 sensillum of the flagellum. Scale bar 2.5 $\mu$ m. (I) Female antenna, trichoid sensillum of the flagellum. Scale bar 10 $\mu$ m.  
391 Inlay: detail of the base of the trichoid sensillum, showing microperforations (arrows). Scale bar 2.5 $\mu$ m. Abbreviations:  
392 BS, basiconic sensillum; CH, chaetic sensillum; FL2, second segment of flagellum; GR, grooved sensillum; PE1, first  
393 segment of pedicel; PE2, second segment of pedicel; SC, scape; TR, trichoid sensillum.  
394

### 395 *H. halys* dsRNA treatment and repellency assay

396 To investigate the functional role of HhTAR1 in *H. halys* behavior and chemosensory recognition  
397 firstly a behavioral repellence assay was set up. *H. halys* 2<sup>nd</sup> instar nymphs were offered a green bean  
398 in the presence or absence of the alarm pheromone component (*E*)-2-decenal and the number of  
399 individuals feeding or standing on the bean was measured during a period of an hour. (*E*)-2-decenal,  
400 as expected, was able to repel approximately 50% of the nymphs compared to the acetone-treated  
401 group, used as control (**Figure 6, panel A**). Subsequently, to assess the physiological relevance of  
402 HhTAR1 in repellency, a RNAi -silencing approach was applied to 2<sup>nd</sup> instar (L2) nymphs. HhTAR1  
403 dsRNA was administered by topical delivery (**Supplementary Figure 4**) to *H. halys* 2<sup>nd</sup> instar  
404 nymphs and the silencing effect on *HhTAR1* transcript levels was evaluated by RT-qPCR 24 h after  
405 the treatment. The dsTAR1 treatment did induce a gene silencing effect, with a 50 % decrease in  
406 transcript abundance while the dsLacZ negative control RNA did not cause any variation (**Figure 6,**  
407 **panel B**). Interestingly, the insects treated the *HhTAR1*-dsRNA exhibited a reduced sensitivity to (*E*-  
408 2-decenal, i.e. they moved towards and fed on green bean in the presence of (*E*)-2-decenal in a similar  
409 manner to the acetone-only control (**Figure 6, panel C**). On the other hand, the behavior of nymphs  
410 treated with *LacZ*-dsRNA was unmodified, therefore the alarm pheromone correctly repelled the  
411 insects (**Figure 6, panel D**).



412

413 **Figure 6.** Olfactory modulation of *H. halys* 2<sup>nd</sup> instar nymphs. (A) Behavioral repellence assay on *H. halys* 2<sup>nd</sup> instar in  
 414 the presence or absence of the alarm pheromone (*E*)-2-decenal. (B) Reduction in *HhTAR1* transcript levels by RNAi.  
 415 Each bar shows the mean fold change  $\pm$  SEM (standard error) of four independent replicates of *H. halys* 2<sup>nd</sup> instar nymphs  
 416 24 h after gene-specific dsRNA treatment, topically delivered. LacZ specific dsRNA treatment was used as a negative  
 417 control. \*\*  $p < 0.01$  vs control according to student's t test. (C) Behavior assay after dsHhTAR1 administration or (D)  
 418 dsLacZ. Data are means  $\pm$  SEM of four independent replicates for a total of at least 50 insect tested. \*  $p < 0.05$  vs control  
 419 according to two-way ANOVA (time x treatment) followed by Dunnett post-hoc.

420

## 421 Discussion

422 Since its appearance in Europe and in America, *Halyomorpha halys* has caused serious damage to  
 423 agriculture (Rice et al., 2014; Valentin et al., 2017). Due to its reduced susceptibility to traditional  
 424 control strategies, new methods for *H. halys* containment need to be developed, identifying innovative  
 425 chemical compounds as well as new targets based on biochemistry, physiology and behavior of this  
 426 insect.

427 This study deal with the molecular and pharmacological characterization of the *H. halys* type 1  
 428 tyramine receptor (*HhTAR1*). Through a RNAi silencing of *HhTAR1*, it was possible to reveal the  
 429 important role of *HhTAR1* in physiological aspects of *H. halys*, such as the olfactory response to the  
 430 alarm pheromone (*E*)-2-decenal.

431 The *HhTAR1* polypeptide shares many structural features with TAR1s from other insect (Ohta &  
 432 Ozoe, 2014). *HhTAR1* contains seven highly conserved transmembrane segments, as expected for a



433 GPCR, as well as phosphorylation and glycosylation sites, typical for this receptor class and essential  
434 for the correct protein folding and receptor signalling (Nørskov-Lauritsen & Bräuner-Osborne, 2015;  
435 Alfonso-Méndez et al., 2017). Most of these sites (seven phosphorylation sites - T<sup>235</sup> and S<sup>246, 260, 294,</sup>  
436 <sup>319, 321, 364</sup>) are localized in the long intracellular loop between TM V and VI and are probably involved  
437 in receptor signalling and regulatory processes such as desensitization and internalization.  
438 Concerning the TA binding site, the main amino acid residue interacting with the endogenous agonist  
439 is an aspartic acid located in TM III and well conserved in all insect TAR1s as judged by alignment  
440 studies (Braza et al., 2019). In HhTAR1 this Asp residue is found at position 128 (D<sup>128</sup>). The D<sup>128</sup>  
441 involvement in ligand binding has been confirmed in a mutation study performed on *Bombyx mori*  
442 TAR1 that showed that the orthologous Asp residue binds the TA-amine group with an ionic bond  
443 reinforced by H-bond (Ohta et al., 2004). The same study also showed that several serine residues in  
444 TM V stabilise the interaction between TAR1 and TA. The HhTAR1 molecular model furthermore  
445 suggests that three serine residues (found at position 212, 213 and 216 and well conserved within  
446 TAR1 insects family) might be involved in generating the receptor binding pocket (Ohta et al., 2004;  
447 Braza et al., 2019).

448 The structural description encouraged to proceed towards a functional characterization. The HhTAR1  
449 coding region was cloned and expressed into HEK 293 cells and the recombinant receptor tested for  
450 its ability to respond to known TAR1 ligands. In the calcium mobilization assay TA was significantly  
451 more potent than OA, as observed for other TAR1s (Gross et al., 2015; Hana & Lange, 2017a; Finetti  
452 et al., 2020). Furthermore, the effect of TA was sensitive to the antagonist yohimbine, as observed in  
453 other orthologous TAR1s (Saudou et al., 1990; Gross et al., 2015; Hana & Lange, 2017a; Finetti et  
454 al., 2020). Other biogenic amines, such as dopamine and adrenaline, were not able to activate  
455 HhTAR1, also shown also in *R. microplus* TAR1 (Gross et al., 2015).

456 Many studies support the physiological role of TAR1 in processes such as locomotion (Saraswati et  
457 al., 2004; Schützler et al., 2019), metabolic control (Nishimura et al., 2005; Li et al., 2017; Roeder,  
458 2020), reproduction (Hana & Lange, 2017a; Hana & Lange, 2017b) and olfaction (Kutsukake et al.,  
459 2000; Brigaud et al., 2009; Duportets et al., 2010; McQuillan et al., 2012; Ma et al., 2015;  
460 Zhukovskaya & Polyakovskiy, 2017; Ma et al., 2019b). The *TAR1* expression patterns mirror its  
461 functional roles because the *TAR1* gene is highly expressed in the CNS, salivary glands and antennae  
462 in different insect species (Duportets et al., 2010; McQuillan et al., 2012; Wu et al., 2014; El-Kholy  
463 et al., 2015; Hana & Lange, 2017a; Ma et al., 2019a; Finetti et al., 2020). Two studies conducted in  
464 2017 on the honeybee brain showed that *TAR1* was mainly expressed at the presynaptic sites in  
465 antennal lobe OSNs and in the mushroom bodies PNs, which are essential structures for the olfactory  
466 system in insects (Synakevitch et al., 2017; Thamm et al., 2017). Similarly, in *H. halys* HhTAR1

467 appeared strongly expressed in brain and antennae, but was less expressed in the midgut and  
468 reproductive systems of adults. Furthermore, *HhTAR1* mRNA was more abundant in the male brain  
469 than in the female one. This sex-dependent *TAR1* expression was also detected in *D. suzukii* (Finetti  
470 et al., 2020) and *P. xylostella* (Ma et al., 2019a) suggesting that TAR1 could be involved in male  
471 specific functions such as development as well as reproduction. The high brain expression of *HhTAR1*  
472 correlates well with the abundance of TAR1 in CNS of numerous insect species (El-Kholy et al.,  
473 2015; Hana & Lange, 2017a; Finetti et al., 2020) where it regulates several sensory processes (Roeder  
474 et al., 2003; Lange, 2009; Ohta & Ozoe, 2014; Neckameyer & Leal, 2017). Interestingly, *HhTAR1*  
475 was also highly abundant in the antennae. As a matter of fact, several studies have shown that *TAR1*  
476 is expressed in these structures even if its role in the antennae is still unclear. A possible correlation  
477 between TAR1 and olfaction was established for the first time in 2000 (Kutsukake et al., 2000). This  
478 study characterized a *D. melanogaster* TAR1-mutant line, called *honoka*, whose behavioral responses  
479 to repellents were reduced in comparison to wild type flies. Our data also revealed that *HhTAR1* is  
480 more expressed in the male antennae of *H. halys* than in female ones. These results suggest that  
481 TAR1, besides being associated with olfactory repellence processes, could also play a role in  
482 responses to olfactory-reproductive stimuli, such as pheromones, or in mating behaviors (Mazzoni et  
483 al., 2017). The *HhTAR1* mRNA resulted more abundant in the two segments of flagellum with a 6-  
484 fold difference in comparison to the other antennal structures. A typical insect antenna contains  
485 numerous sensilla, essential structures for smell, taste, mechanoreception and thermo-hygro  
486 perception (Zacharuk, 1985). The great number of sensilla in the apical parts of the *H. halys* antennae  
487 correlates with the high *HhTAR1* expression level in the same areas, further strengthening a role for  
488 TAR1 in olfaction. Since the physiological role of each sensilla may be predicted based on their  
489 morphology, size and distribution (Keil, 1999), the *H. halys* sensilla were investigated by SEM.  
490 Different types of sensilla have been classified in the Pentatomidae, including basiconic, trichoid,  
491 coeloconic and chaetic sensilla (Brèzot et al., 1997). The most abundant structures in FL1 and FL2  
492 segments of the adult *H. halys* were trichoid sensilla (TR) followed basiconic sensilla (BS) or  
493 “grooved sensilla” as observed also by Ibrahim et al. (2019) in the same insect. Both TR and BS-C  
494 share olfactory functions (Toyama et al., 2006) as suggested by the presence, on the surface, of  
495 distinctive microperforations necessary to connect the odorous molecules with the olfactory receptors  
496 in the OSNs (Zacharuk, 1985). It is difficult to associate each type of sensillum to a specific olfactory-  
497 mediated behavior, but the removal of both FLs completely inhibited the adult *H. halys* aggregation,  
498 indicating that these structures, and probably also TR and BS are necessary to perceive the  
499 aggregation pheromone (Toyama et al., 2006). On the other hand, sporadic BS have been observed  
500 in SC and both PEs along with structures identified as pit sensilla or coeloconic sensilla that could be

501 involved in the thermo-hygrosensory reception (Altner & Prillinger, 1980). It is interesting to note  
502 that *HhTAR1* is more expressed in the FLs as compared to the SC and both Pes suggesting a  
503 correlation between TAR1 and olfactory sensilla. These data would therefore lead to hypothesize an  
504 important role for HhTAR1 in olfactory processes. Interestingly, *HhTAR1* showed high expression  
505 levels also in eggs and in 1<sup>st</sup> and 2<sup>nd</sup> instar nymphs, followed by a dramatic decrease from the 3<sup>rd</sup>  
506 instar nymphs onwards. The results also revealed that between 2<sup>nd</sup> and 3<sup>rd</sup> instar nymphs the *HhTAR1*  
507 expression decreased more (about 80 %) in the abdomen and thorax tissues in comparison to the head.  
508 Also in adults, *HhTAR1* levels remained high in brain and antennae in comparison to other tissues.  
509 Previous studies observed that *H. halys* nymphs exhibit 4-times higher mortality than adults after  
510 treatment with essential oils for 1 or 48 h (Bergmann & Raupp, 2014) The high *HhTAR1* expression  
511 in CNS and antennae nymphs might explain the greater sensitivity to volatile compounds with  
512 insecticides properties, such as essential oils. In fact, TAR1 is a putative target for biopesticides, such  
513 as monoterpenes (Gross et al., 2017, Finetti et al., 2020). It is not yet clear how monoterpenes exert  
514 their toxicity in vertebrates, but their volatile nature is currently used to repel various insect pests  
515 (Reis et al., 2016).

516 The analysis on *HhTAR1* expression patterns together with the SEM observations on *H. halys*  
517 antennae strongly suggest a connection between HhTAR1 and *H. halys* olfactory regulation. To better  
518 investigate this aspect, *HhTAR1* was silenced by RNAi in young nymphs. In recent years, several  
519 Hemiptera genes have been successfully silenced through this method (Christiaens & Smaghe, 2014;  
520 Bansal et al., 2016; Ghosh et al., 2017; Lu et al., 2017; Mogilicherla et al., 2018, Riga et al., 2019).  
521 In these studies, the dsRNA was delivered exclusively by microinjection or by feeding but both these  
522 delivery methods are problematic. Microinjection requires experience and specific instruments to  
523 control the injected volume, as well as minimizing the wound that often causes a drastic increasing  
524 in mortality (Christiaens et al., 2020). In fact, through the microinjection we were able to obtain a  
525 *HhTAR1* RNAi downregulation in *H. halys* 2<sup>nd</sup> instar nymphs (data not shown) but with an extremely  
526 high mortality. On the other hand, the dsRNA delivery by feeding requires a large amount of dsRNA  
527 and it does not allow to control the amount of dsRNA ingested by each insect (Joga et al., 2016). The  
528 dsRNA topical delivery has been recently tested in two Hemiptera species, *Diaphorina citri* and  
529 *Acyrtosiphon pisum*. In *D. citri*, 20 ng of dsRNA solution topically delivered on the abdomen were  
530 able to silence several *Cyp* genes by about 70-90% (Killiny et al., 2014). In *A. pisum*, 120 ng of  
531 dsRNA solution induced a downregulation of a target gene by 90 % after 24-36 hours (Niu et al.,  
532 2019). Accordingly, in *H. halys* 2<sup>nd</sup> instar nymphs (rich in *HhTAR1* mRNA), a 100 ng dose of  
533 *HhTAR1* dsRNA topically delivered appeared sufficient to silence *HhTAR1* by about 50 % after 24  
534 hours, as verified by RT-qPCR. The different RNAi efficiency observed between *D. citri*, *A. pisum*

535 and *H. halys* could be explained to the different body structure: the abdominal cuticle of *H. halys*  
536 nymphs is thicker than that of *D. citri* and *A. pisum*, an aspect that could limit absorption of dsRNA  
537 solution. At any rate, this is the first time that RNAi mediated gene silencing is induced by topic  
538 delivery in *H. halys*. In previous studies, RNAi silencing has already been successfully performed on  
539 this insect using microinjection and feeding as delivery methods. One  $\mu\text{g}$  of dsRNA injected in *H.*  
540 *halys* adults was able to silence several target genes by 60-80 % after 72 h (Mogilicherla et al., 2018).  
541 On the contrary, when the dsRNA solution was delivered by feeding to *H. halys* 2<sup>nd</sup> and 4<sup>th</sup> instar  
542 nymphs, some target genes were silenced only by 40 - 80 % (Kumar et al., 2017). Although the  
543 dsRNA topically delivered results less efficient as gene silencer in *H. halys*, the administered amount  
544 of dsRNA is lower compared to the microinjection and the feeding applications. Reducing the dsRNA  
545 amount could be an effective strategy to prevent off target effects (Romeis & Widmer, 2020).  
546 Upon *HhTAR1* silencing, *H. halys* 2<sup>nd</sup> instar nymphs were tested in their olfactive performances by  
547 an innovative behavioral assay. This assay measured the repellent effect of (*E*)-2-decenal, one of the  
548 main alarm compounds released by *H. halys* under threats, on 2<sup>nd</sup> instar nymphs (Zhong et al., 2017;  
549 Zhong et al. , 2018; Nixon et al., 2018). The *HhTAR1*-dsRNA treatment caused a reduced sensitivity  
550 to (*E*)-2-decenal in comparison to the *LacZ*-dsRNA control nymphs. suggesting that the (*E*)-2-  
551 decenal-mediated alarm requires a functional TAR1.  
552 In conclusion, *HhTAR1* could play a relevant role in the *H. halys* olfactory network, contributing to  
553 modulate olfaction-mediated behaviors, such as reception of alarm pheromone compounds. A more  
554 detailed characterization of the interconnections between TAR1 and the olfactory system will pave  
555 the way for developing TAR1-targeting volatile compounds, such as essential oils, with both repellent  
556 and insecticidal properties against *H. halys*.

557

## 558 **Acknowledgement**

559 The authors would like to thank Dott. Santolo Francati (University of Bologna) for providing *H. halys*  
560 adults, Dott.ssa Morena De Bastiani (University of Ferrara) for the technical assistance, Prof. Stefano  
561 Della Longa (University of L'Aquila) and Prof. Alessandro Arcovito (Università Cattolica del Sacro  
562 Cuore, Rome) for molecular modelling advice, Dott.ssa Federica Albanese (University of Ferrara)  
563 and Dott.ssa Milvia Chicca (University of Ferrara) for language revision.

564 This study was funded by 'Camera di Commercio Industria, Artigianato e Agricoltura' of Ferrara  
565 'Bando 2018' and by the Emilia Romagna region within the Rural Development Plan 2014-2020 Op.  
566 16.1.01 – GO EIP-Agri - FA 4B, Pr. “ALIEN.STOP”, coordinated by CRPV.

567

## 568 **References**

- 569  
570 Alfonzo-Méndez, M.A., Alcántara-Hernández, R & García-Sàinz, J.A. (2017). Novel structural approaches to study GPCR regulation. *International*  
571 *Journal of Molecular Sciences*, 18, 27.  
572  
573 Altner, H. & Prillinger, L. (1980). Ultrastructure of invertebrate chemo, thermo, and hygroreceptors and its functional significance. *International Review*  
574 *of Cytology*, 67, 69-139.  
575  
576 Amin, H. & Lin, C.A. (2019). Neuronal mechanisms underlying innate and learned olfactory processing in *Drosophila*. *Current Opinion in Insect*  
577 *Science*, 36, 9-17.  
578  
579 Bansal, R., Mittaperry, P., Chen, Y., Mamidal, P., Zhao, C. & Michel, A. (2016). Quantitative RT-PCR gene evaluation and RNA interference in the  
580 Brown Marmorated Stink Bug. *PLoS One*, 4, 11(5), e0152730.  
581  
582 Bayliss, A., Roselli, G. & Evans, P.D. (2013). A comparison of the signalling properties of two tyramine receptor from *Drosophila*. *Journal of*  
583 *Neurochemistry*. 125(1): 37-48.  
584  
585 Bergmann, E. & Raupp, M. (2014). Efficacies of common ready to use insecticides against *Halyomorpha halys* (Hemipter: Pentatomidae). *Florida*  
586 *Entomologist*, 97(2), 791-800.  
587  
588 Blenau, W., Balfanz, S. & Baumann, A. (2000). Amtyr1: Characterization of a gene from honeybee (*Apis mellifera*) brain encoding a functional tyramine  
589 receptor. *Journal of Neurochemistry*, 74(3), 900-908.  
590  
591 Blenau, W. & Baumann, A. (2003). Aminergic signal transduction in invertebrates: focus on tyramine and octopamine receptors. *Recent Research*  
592 *Developments in Neurochemistry*, 6, 225-240.  
593  
594 Braza, M.K.E., Gazmen, J.D.N., Yu, E.T. & Nellas, R.B. (2019). Ligand-induced conformational dynamics of a tyramine receptor from *Sitophilus*  
595 *oryzae*. *Scientific Reports*, 9, 16275.  
596  
597 Brèzot, P., Taudan, D. & Renon, M. (1997). Sense organs on the antennal flagellum of the green stink bug, *Nezara viridula* (L.) (Heteroptera:  
598 Pentatomidae): sensillum types and numerical growth during the post-embryonic development. *International Journal of Insect Morphology and*  
599 *Embryology*, 25, 427-441.  
600  
601 Brigaud, L., Grosmaître, X., François, M. C. & Jacqion-Joly, E. (2009). Cloning and expression pattern of a putative octopamine/tyramine receptor in  
602 antennae of the noctuid moth *Mamestra brassicae*. *Cell Tissue Research*, 335, 445-463.  
603  
604 Carey, A.F. & Carlson, J.R. (2011). Insect olfaction from model systems to disease control. *Proceedings of the National Academy of Sciences*, 108,  
605 12987-12995.  
606  
607 Caron, S.J.C., Ruta, V., Abbott, L.F. & Axel, R. (2013). Random convergence of olfactory inputs in the *Drosophila* mushroom body. *Nature*, 497: 113-  
608 117.  
609  
610 Cesari, M., Maistrello, L., Piemontese, L., Bonini, R., Dioli, P., Lee, W., Park, C-G., Partsinevelos, G. K., Rebecchi, L. & Guidetti, R. (2018). Genetic  
611 diversity of the Brown Marmorated Stink Bug *Halyomorpha halys* in the invaded territories of Europe and its patterns of diffusion in Italy. *Biological*  
612 *Invasions*, 20, 1073-1092.  
613  
614 Chenn, V.B., Arendall, W.B., Headd, J.J., Keedy, D.A., Immormino, R.M., Kapral, G.J., Murray, L.W., Richardson, J.S. & Richardson, D.C. (2010).  
615 *Acta Crystallographica*, 66: 16-21.  
616  
617 Christiaens, O. & Smaghe, G. (2014). The challenge of RNAi-mediated control of hemipterans. *Current Opinion in Insect Science*, 6:15-21.  
618  
619 Christiaens, O., Whyard, S., Vèlez, A.M & Smaghe, G. (2020). Double-stranded RNA technology to control insect pest: current status and challenges.  
620 *Frontiers in Plant Science*, 11: 451.  
621  
622 Duportets, L., Barrozo, R.B., Bozzolan, F., Gaertner, C., Anton, S., Gadenne, C. & Debernard, S. (2010). Cloning of an octopamine/tyramine receptor  
623 and plasticity of its expression as a function of adult sexual maturation in the male moth *Agrotis ipsilon*. *Insect Molecular Biology*, 19(4), 489-499.  
624  
625 El-Kholy, S., Stephano, F., Li, Y., Bhandari, A., Fink, C. & Roeder, T. (2015). Expression analysis of octopamine and tyramine receptors in *Drosophila*.  
626 *Cell and Tissue Research* 361(3), 669-684.  
627  
628 Enan, E.E. (2005). Molecular response of *Drosophila melanogaster* tyramine receptor cascade to plant essential oils. *Insect Biochemistry and Molecular*  
629 *Biology*, 35, 309-321.  
630  
631 Finetti, L., Ferrari, F., Cassaneli, S., De Bastiani, M., Civolani, S. & Bernacchia, G. (2020). Modulation of *Drosophila suzukii* type 1 tyramine receptor  
632 (DsTAR1) by monoterpenes: a potential new target for next generation biopesticides. *Pesticide Biochemistry and Physiology*, 165, 104549.  
633  
634 Gadenne, C., Barrozo, R.B. & Anton, S. (2016). Plasticity in insect olfaction: to smell or not to smell? *Annual Review of Entomology* 61, 317-333.

- 635  
636 Ghosh, S.K.B., Hunter, W.B., Park, A.L. & Gundersen-Rindal, D.E. (2017). Double strand RNA delivery system for plant-sap-feeding insects. *PLoS*  
637 *ONE*, 12(2): e0171861.  
638  
639 Gross, A.D., Temeyer, K.B., Day, T.A., Pérez de León, A.A., Kimber, M.J. & Coats, J.R. (2015). Pharmacological characterization of a tyramine  
640 receptor from the southern cattle tick, *Rhipicephalus (Boophilus) microplus*. *Insect Biochemistry and Molecular Biology*, 63, 47-53.  
641  
642 Gross, A.D., Temeyer, K.B., Day, T.A., Pérez de León, A.A., Kimber, M.J. & Coats J.R. (2017). Interaction of plant essential oil terpenoids with the  
643 southern cattle tick tyramine receptor: A potential biopesticide target. *Chemico-Biological Interactions*, 263, 1-6.  
644  
645 Hana, S. & Lange A.B. (2017a). Cloning and functional characterization of Oct $\beta$ 2-receptor and Tyr1-receptor in the chagas disease vector, *Rhodnius*  
646 *prolixus*. *Frontiers in Physiology*, 8, 744.  
647  
648 Hana, S. & Lange A.B. (2017b). Octopamine and tyramine regulate the activity of reproductive visceral muscles in the adult female blood-feeding bug,  
649 *Rhodnius prolixus*. *Journal of Experimental Biology*, 220, 1830-1836.  
650  
651 Haye, T., Garipey, T.D., Hoelmer, K., Rossi, J.P., Streito, J.C., Tassus, T. & Desneux, N. (2015). Range expansion of the invasive Brown Marmorated  
652 Stink Bug, *Halyomorpha halys*: an increasing threat to field, fruit and vegetable crops worldwide. *Journal of Pest Science*, 88, 665-673.  
653  
654 Hoebeke, E.R. & Carter, M.E. (2003). *Halyomorpha halys* (Stål) (Heteroptera: Pentatomidae): A polyphagous plant pest from Asia newly detected in  
655 North America. *Proceedings - Entomological Society of Washington*, 105(1), 225-237.  
656  
657 Ibrahim, A., Giovannini, I., Anfora, G., Rossi Stacconi, M.V., Malek, R., Maistrello, L., Guidetti, R. & Romani, R. (2019). A closer look at the antennae  
658 of the invasive *Halyomorpha halys*: fine structure of the sensilla. *Bulletin of Insectology*, 72(2), 187-199.  
659  
660 Jefferis, G.S.X.E., Potter, C.J., Chan, A.M., et al. (2007). Comprehensive maps of *Drosophila* higher olfactory centers: spatially segregated fruit and  
661 pheromone representation. *Cell*, 128, 1187-1203.  
662  
663 Joga, M.R., Zotti, M.J., Smaghe, G. & Christiaens, O. (2016). RNAi efficiency, systemic properties, and novel delivery methods for pest insect control:  
664 what we know so far. *Frontiers in Physiology*, 7:553.  
665  
666 Keil, T.A. (1999). Morphology and development of the peripheral olfactory organs, pp. 5-47. In: *Insect Olfaction* (Hansson B. S., Ed.) - Springer,  
667 Berlin, Germany.  
668  
669 Kenakin, T.A. (2014). *Pharmacology Primer 4<sup>th</sup> Edition*. Techniques for more effective and strategic drug discovery. Elsevier Science Publishing Co.  
670 Inc. 525B Street, Suite 1800, San Diego, CA 92101-4495, USA.  
671  
672 Killiny, N., Hajeri, S., Tiwari, S., Gowda, S. & Stelinski, L.L. (2014). Double-stranded RNA uptake through topical application, mediates silencing of  
673 five CYP4 genes and suppresses insecticide resistance in *Diaphorina citri*. *PLoS ONE*, 9(10): e110536.  
674  
675 Kumar, R. (2019). Molecular markers and their application in the monitoring of acaricide resistance in *Rhipicephalus microplus*. *Experimental and*  
676 *Applied Acarology* 78: 149-172.  
677  
678 Kutsukake, M., Komatsu, A., Yamamoto, D. & Ishiwa-Chigusa, S. (2000). A tyramine receptor gene mutation causes a defective olfactory behaviour  
679 in *Drosophila melanogaster*. *Gene* 245, 31-42.  
680  
681 Kyte, A. & Doolittle, F.R. (1982). A simple method for displaying the hydrophobic character of a protein. *Journal of Molecular Biology*, 157, 105-132.  
682  
683 Lange, A.B. (2009). Tyramine: from octopamine precursor to neuroactive chemical in insects. *General and Comparative Endocrinology*, 162, 18-26.  
684  
685 Larionov, A., Krause, A. & Miller, W. (2005). A standard curve-based method for relative real time PCR data processing. *BMC Bioinformatics*. 21, 6,  
686 62.  
687  
688 Lee, D-H., Short, B.D., Joseph, S.V., Bergh, J.C. & Leskey, T.C. (2013). Review of the biology, ecology and management of *Halyomorpha halys*  
689 (Hemiptera: Pentatomidae) in China, Japan, and the Republic of Korea. *Environmental Entomology*, 42(4), 627-641.  
690  
691 Leskey, T.C. & Nielsen, A.L. (2018). Impact of the Brown Marmorated Stink Bug in North America and Europe: history, biology, ecology and  
692 management. *Annual Review of Entomology*, 63(1), 599-608.  
693  
694 Li, Y., Tiedemann, L., Von Frieling, J., Nolte, S., El-Kholy, S., Stephano, F., Gelhaus, C., Bruchhaus, I., Fink, C. & Roeder, T. (2017). The Role of  
695 Monoaminergic Neurotransmission for Metabolic Control in the Fruit Fly *Drosophila melanogaster*. *Frontiers in Systems Neuroscience*, 11, 60.  
696  
697 Lu, Y., Chen, M., Reding, K. & Pick, L. (2017). Establishment of molecular genetic approaches to study gene expression and function in an invasive  
698 hemipteran, *Halyomorpha halys*. *EvoDevo*, 8:15.  
699  
700 Ma, Z., Guo, X., Lei, H., Li, T., Hao, S. & Kang, L. (2015). Octopamine and tyramine respectively regulate attractive and repulsive behavior in locust  
701 phase changes. *Scientific Reports*, 5: 8036.

702  
703 Ma, H., Huang, Q., Lai, X., Liu, J., Zhu, H., Zhou, Y., Deng, X. & Zhou, X. (2019a). Pharmacological properties of the type 1 tyramine receptor in the  
704 Diamondback moth, *Plutella xylostella*. *International Journal of Molecular Sciences*, 20, 2953.  
705  
706 Ma, Z., Guo, X. & Liu, J. (2019b). Trasllocator protein mediates olfactory repulsion. *The FASEB Journal*, 34(1): 513-524.  
707  
708 Mazzoni, V., Polajnar, J., Baldini, M., Stacconi, M.V.R., Anfora, G., Guidetti, R. & Maistrello, L. (2017). Use of substrate-borne vibrational signals to  
709 attract the brown marmorated stink bug, *Halyomorpha halys*. *Journal of Pest Science*, 90, 1219-1229.  
710  
711 McQuillan, H.J., Barron, A.B. & Mercer, A.R. (2012). Age- and behaviour-related changes in the expression of biogenic amine receptor genes in the  
712 antennae of honeybees (*Apis mellifera*). *Journal of Comparative Physiology A*, 198, 753-761.  
713  
714 Mogilicherla, K., Howell, J.L. & palli, S.R. (2018). Improving RNAi in the brown marmorated stink bug: identification of target genes and reference  
715 genes for RT-qPCR. *Scientific Reports*, 8:3720.  
716  
717 Neckameyer, W.S. & Leal, S.M. (2017). Diverse functions of insect biogenic amines as neurotransmitters, neuromodulators and neurohormones.  
718 *Hormones, Brain and Behavior*, 3<sup>rd</sup> edn, Academic Press, Oxford, 368-400.  
719  
720 Nielsen, A.L., Chen, S.F. & Fleischer, S.J. (2016). Coupling, developmental, physiology, photoperiod and temperature to model phenology and  
721 dynamics of an invasive Heteropteran, *Halyomorpha halys*. *Frontiers in Physiology*, 7, 165.  
722  
723 Nishimura, T., Seto, A., Nakamura, K., Miyama, M., Nagao, T., Tamotsu, S., Yamaoka, R. & Ozaki, M. (2005). Experiential effects of appetitive and  
724 nonappetitive odors on feeding behavior in the blowfly, *Phormia regina*: a putative role for tyramine in appetite regulation. *Journal of Neuroscience*,  
725 25, 7507-7516.  
726  
727 Niu, J., Yang, W.-J., Tian, Y., Fan, J.-Y., Ye, C., Shang, F., Ding, B.-Y., Zhang, J., An, X., Yang, L., Chang, T.-Y., Christiaens, O., Smagghe, G. & Wang,  
728 J.-J. (2019). Topical dsRNA delivery induces gene silencing and mortality in the pea aphid. *Pest Management Science*, 75(11): 2873-2881.  
729  
730 Nixon, L.J., Morrison, W.R., Rice, K.B., Brockerhoff, E.G., Leskey, T.C., Guzman, F., Khirman, A., Goldson, S. & Rostàs, M. (2018). Identification  
731 of volatiles released by diapausing brown marmorated stink bug, *Halyomorpha halys* (Hemiptera: Pentatomidae). *PLoS ONE*, 13(1): e0191223.  
732  
733 Nørskov-Lauritsen, L. & Bräuner-Osborne, H. (2015). Role of post-translational modifications on structure, function and pharmacology of class C G  
734 protein-coupled receptors. *European Journal of Pharmacology*, 15, 763 (Pt B), 233-40.  
735  
736 Ocampo, A.B., Braza, M.K.E. & Nellas, R.B. (2020). The interaction and mechanism of monoterpenes with tyramine receptor (SoTyr) of rice weevil  
737 (*Sitophilus oryzae*). *SN Applied Sciences*, 2: 1592.  
738  
739 Ohta, H., Utsumi, T. & Ozoe, Y. (2003). B96Bom encodes a *Bombyx mori* tyramine receptor negatively coupled to adenylate cyclase. *Insect Molecular*  
740 *Biology*, 12(3), 217-23.  
741  
742 Ohta, H., Utsumi, T. & Ozoe, Y. (2004). Amino acid residues involved in interaction with tyramine in the *Bombyx mori* tyramine receptor. *Insect*  
743 *Molecular Biology*, 13, 531-538.  
744  
745 Ohta, H. & Ozoe, Y. (2014). Molecular signalling, pharmacology, and physiology of octopamine and tyramine receptors as potential insect pest control  
746 targets. *Advances in Insect Physiology*, 46, chapter two.  
747  
748 Peiffer, M. & Felton, G.W. (2014). Insights into the saliva of the Brown Marmorated Stink Bug *Halyomorpha halys* (Hemiptera: Pentatomidae). *PLoS*  
749 *One*, 26,9(2),e88483.  
750  
751 Pezzi, M., Cultrera, R., Chicca, M., Leis, M. (2015). Scanning electron microscopy investigations of third-instar larva of *Cordylobia rodhaini* (Diptera:  
752 Calliphoridae), an agent of furuncular myiasis. *Journal of Medical Entomology*, 52, 368-374.  
753  
754 Pezzi, M., Whitmore, D., Chicca, M., Semeraro, B., Brighi, F., Leis M. (2016). Ultrastructural morphology of the antenna and maxillary palp of  
755 *Sarcophaga tibialis* (Diptera: Sarcophagidae). *Journal of Medical Entomology*, 53, 807-814.  
756  
757 Poels, J., Suner, M.M., Needham, M., Torfs, H., De Rijck, J., De Loof, A., Dunbar, S.J. & Vanden Broeck, J. (2001). Functional expression of a locust  
758 tyramine receptor in murine erythroleukaemia cells. *Insect Molecular Biology*, 10(6), 541-8.  
759  
760 Reis, S.L., Mantello, A.G., Macedo, J.M., Gelfuso, E.A., da Silva, C.P., Fachin, A.L., Cardoso, A.M. & Belebony, R.O. (2016). Typical monoterpenes  
761 as insecticides and repellents against stored grain pests. *Molecules*, 21, 258.  
762  
763 Rice, K.B., Bergh C.J., Bergmann, E.J., Biddinger, D.J., Dieckhoff, C., Dively, G., Fraser, H., Garipey, T., Hamilton, G., Haye, T., Herbert, A., Hoelmer,  
764 K., Hooks, C.R., Jones, A., Krawczyk, G., Kuhar, T., Martinson, H., Mitchell, W., Nielsen, A.L., Pfeiffer, D.G., Raupp, M.J., Rodriguez-Saona, C.,  
765 Shearer, P., Shrewsbury, P., Venugopal, P.D., Whalen, J., Wiman, N.G., Leskey, T.C. & Tooker, J.F. (2014). Biology, Ecology, and Management of  
766 Brown Marmorated Stink Bug (Hemiptera: Pentatomidae). *Journal of Integrated Pest Management*, 5(3), 1-13.  
767

- 768 Riga, M., Deneck, S., Livadaras, I., Geibel, S., Nauen, R. & Vontas, J. (2019). Development of efficient RNAi in *Nezara viridula* for use in insecticide  
769 target discovery. *Archives of Insect Biochemistry and Physiology*, e21650.  
770
- 771 Roeder, T., Seifert, M., Kähler, C. & Gewecke, M. (2003). Tyramine and octopamine: antagonist modulators of behavior and metabolism. *Archives of*  
772 *Insect Biochemistry and Physiology*, 54, 1-13.  
773
- 774 Roeder, T. (2005). Tyramine and octopamine: ruling behaviour and metabolism. *Annual Review of Entomology*, 50, 447-477.  
775
- 776 Roeder, T. (2020). The control of metabolic traits by octopamine and tyramine in invertebrates. *Journal of Experimental Biology*, 223, jeb194282.  
777
- 778 Romeis, J. & Widmer, F. (2020). Assessing the risk of topically applied dsRNA-based products to non-target arthropods. *Frontiers in Plant Science*,  
779 11:679.  
780
- 781 Rotte, C., Krach, C., Balfanz, S., Baumann, A., Walz, B. & Blenau, W. (2009). Molecular characterization and localization of the first tyramine receptor  
782 of the American cockroach (*Periplaneta americana*). *Neuroscience*, 162, 1120-1133.  
783
- 784 Rouhana, L., Weiss, J.A., Forsthoefel, D.J., Lee, H., King, R.S., Inoue, T., Shibata, N., Agata, K. & Newmark, P.A. (2013). RNA interference by feeding  
785 in vitro synthesized double-stranded RNA to planarians: methodology and dynamics. *Developmental Dynamics*, 242(6): 718-730.  
786
- 787 Saraswati, S., Fox, L.E., Soll, D.R. & Wu, C-F. (2004). Tyramine and octopamine have opposite effects on the locomotion of *Drosophila* larvae. *Journal*  
788 *of Neurobiology*, 58(4), 425-41.  
789
- 790 Saudou, F., Amlaiky, N., Plassat, J.L., Borrelli, E. & Hen, R. (1990). Cloning and characterization of a *Drosophila* tyramine receptor. *The EMBO*  
791 *Journal*, 9(11), 3611-3617.  
792
- 793 Schützler, N., Girwert, C., Hügli, I., Mohana, G., Roignant, J-Y, Ryglewski, S. & Duch, C. (2019). Tyramine action on motoneuron excitability and  
794 adaptable tyramine/octopamine ratios adjust *Drosophila* locomotion to nutritional state. *Proceedings of the National Academy of Sciences*, 116(9),  
795 3805-3810.  
796
- 797 Synakevitch, I.T., Daskalova, S.M. & Smith, H. (2017). The biogenic amine tyramine and its receptor (AmTyr1) in olfactory neuropils in the honeybee  
798 (*Apis mellifera*) brain. *Frontiers in System Neuroscience*, 11:77.  
799
- 800 Tanaka, N.K., Suzuki, E., Dye, L., Ejima, A. & Stopfer, M. (2012). Dye fills reveal additional olfactory tracts in the protocerebrum of wild-type  
801 *Drosophila*. *Journal of Comparative Neurology*, 520, 4131-4140.  
802
- 803 Thamm, M., Scholl, C., Reim, T., Grübel, K., Moller, K., Rossler, W. & Scheiner, R. (2017). Neuronal distribution of tyramine and the tyramine  
804 receptor AmTAR1 in the honeybee brain. *Journal of Comparative Neurology*, 525, 2615-2631.  
805
- 806 Toyama, M., Ihara, F. & Yaginuma, K. (2006). Formation of aggregations in adults of the brown marmorated stink bug, *Halyomorpha halys* (Stål)  
807 (Heteroptera: Pentatomidae): the role of antennae in short-range locations. *Applied Entomology and Zoology*, 41, 309-315.  
808
- 809 Valentin, R.E., Nielsen, A.L., Wiman, N.G., Lee, D-H. & Fonseca, D.M. (2017). Global invasion network of the brown marmorated stink bug,  
810 *Halyomorpha halys*. *Scientific Reports*: 7.  
811
- 812 Waterhouse, A., Bertoni, M., Bienert, S., Studer, G., Tauriello, G., Gumienny, R., Heer, F.T., de Beer, T.A.P., Rempfer, C., Bordoli, L., Lepore, R. &  
813 Schwede, T. (2018). SWISS-MODEL: homology modelling of protein structures and complexes. *Nucleic Acids Research*, 46: 296-303.  
814
- 815 Wu, S.F., Xu, G., Qi, Y.X., Xia, R.Y., Huang, J. & Ye, G.Y. (2014). Two splicing variants of a novel family of octopamine receptors with different  
816 signalling properties. *Journal of Neurochemistry*, 129, 37-47.  
817
- 818 Zacharuk, R.Y. (1985). Antennae and sensilla. *Comprehensive Insect Physiology, Biochemistry and Pharmacology* (Kerkut G.A., Gilbert L.I. Eds), vol.  
819 6, 1-69.  
820
- 821 Zhao, Z. & McBride, C.S. (2020). Evolution of olfactory circuits in insects. *Journal of Comparative Physiology A*, 206, 353-367.  
822
- 823 Zhong, Z-Z., Tang, R., Zhang, J-P., Yang, S-Y., Chen, G-H., He, K-L., Wang, Z-Y. & Zhang, F. (2018). Behavioral evidence and olfactory reception  
824 of a single alarm pheromone component in *Halyomorpha halys*. *Frontiers in Physiology*, 9:1610.  
825
- 826 Zhong, Z-Z., Zhang, J-P., Ren, L-L., Tang, R., Zhang, H-X., Chen, G-H. & Zhang, F. (2017). Behavioral responses of the egg parasitoid *Trissolcus*  
827 *japonicus* to volatiles from adults of its stink bug host, *Halyomorpha halys*. *Journal of Pest Science*, 90: 1097-1105.  
828
- 829 Zhukovskaya, M.I. & Polyanovsky, A.D. (2017). Biogenic amines in insect antennae. *Frontiers in Systems Neuroscience*. 11, 45.  
830  
831  
832



833 **Table 1.** Primers used in this study.

Primer	Primer sequence (5'-3')
Cloning	
<i>HhTARI-Fw</i>	TTAGTGCGGTGAGGAAGGTT
<i>HhTARI-Fw-Kozak</i>	GCCACCATGGAGTGGACTATAGAG
<i>HhTARI-Rev</i>	CGATTTTCATGGAGAAGTGGA
RT-qPCR analysis	
<i>HhTARI-Fw</i>	CTCATTGGCTGGAACGACTG
<i>HhTARI-Rev</i>	CCCGTTCACGTAACCTCCTC
<i>ARP8-Fw</i>	TTGATGCTGACTGGCCCTAA
<i>ARP8-Rev</i>	GGCCTCCTTCGTTGGTACAG
<i>UBE4A-Fw</i>	CGCCAGCTGACTTTTCCTCT
<i>UBE4A-Rev</i>	GACAGCAGTGGCTCCATCAG
dsRNA synthesis	
<i>HhTARI-Fw</i>	GAATTAATACGACTCACTATAGGGAGACCGGAAGTCTTCAGCAACT
<i>HhTARI-Rev</i>	GAATTAATACGACTCACTATAGGGAGACGTGACTTAGGGGAATTGG
<i>LacZ-Fw</i>	GAATTAATACGACTCACTATAGGGAGATGAAAGCTGGCTACAGGA
<i>LacZ-Rev</i>	GAATTAATACGACTCACTATAGGGAGAGCAGGCTTCTGCTTCAAT

834

835

836 **Table 2.** MolProbity results based on the HhTAR1 3D model obtained by SWISS-MODEL software.  
837

<b>MolProbity Parameter</b>	<b>Result</b>
MolProbity Score	1.95
ClashScore	3.07 (M <sup>260</sup> , K <sup>263</sup> )
Ramachandran Favoured	97.94 % (goal: > 98 %)
Ramachandran Outliers	0.51 % (D <sup>331</sup> , P <sup>77</sup> ) (goal: < 0.2 %)

838  
839

840 **Supplementary Figure 1 (S1)**

841

```

1 - 66   ATGGAGTGGGACTATAGAGACAACCTGTACAACGGAACCAACGGAAGCCTTTTGGCAGACCGAAAC
1 - 22   M E W D Y R D N L Y N G T N G S L L A D R N
67 - 132 GGTAGTTGCCCTAAGACCAGCACCTGTTCATGAGACTCCCTTCGGAGTGGCCTTCGCAGTACCG
23 - 44   G S C P K T S T L F H E T P F G V A F A V P
133 - 198 ATCTGGGAAGGAATATCCACGGCGATCGTCTCACTCTGATCATCATCTTTACCATCGTGGGCAAC
45 - 66   I W E G I S T A I V L T L I I I F T I V G N
199 - 264 ATCTTGGTCATTTCTCAGTGTCTTCACTTACAAACCACTCCGGATCGTACAAAACCTTTCATAGTC
67 - 88   I L V I L S V F T Y K P L R I V Q N F F I V
265 - 330 AGCCTTGCAGTGGCCGACCTGACGGTTGCAATCTTGGTGCTGCCTTTCAACGTGGCTTACTCTATA
89 - 110   S L A V A D L T V A I L V L P F N V A Y S I
331 - 396 CTAGGTCGCTGGGTGTTTGAATCCACATTTGCAAGATGTGGCTGACCAGTGACGTATGTGCTGT
111 - 132   L G R W V F G I H I C K M W L T S D V M C C
397 - 462 ACTGCATCAATTTCTCAATTTGTGCCTATTTGCCCTCGATAGGTAAGTGGCCATTACAGACCCTATT
133 - 154   T A S I L N L C A I A L D R Y W A I T D P I
463 - 528 AAATATGCCCAAAAAGGACACTGAAGAGAGTTCCTCGTATGATCGCGGGGTCTGGATAATGTCA
155 - 176   N Y A Q K R T L K R V L V M I A G V W I M S
529 - 594 ATGTTGATCAGCTCACCACTCTCATTGGCTGGAACGACTGGCCGGAAGTCTTACCAACTCCACA
177 - 198   M L I S S P P L I G W N D W P E V F S N S T
595 - 660 CCATGCCAGCTCACTTCTCAGCAGGGTTACGTAATATATTCGTCCTTAGGCTCCTTTTACATCCCT
199 - 220   P C Q L T S Q Q G Y V I Y S S L G S F Y I P
661 - 726 CTGTTCACTATGACGATTGTTTACATAGAAATATTTATAGCCACCAGGAGGTTACGTGAACGG
221 - 242   L F T M T I V Y I E I F I A T R R R L R E R
727 - 792 GCTAGAGCGTCTAAACTCAATGCTGTAAAACAAAACCTTACAACAGAACAAATCAATGAGAGAGAAG
243 - 264   A R A S K L N A V K Q N L Q Q N N S M R E K
793 - 858 CATTACCCGATTGATGGTGAATCAGTGAGCAGTGAGAATGCTAATGAAGAACACCAAGGAAAAGAG
265 - 286   H S P I D G E S V S S E N A N E E H K E K K
859 - 924 AAAAGAAGAAGAAGAAAAATCAGAAGAAAAGAAGAACCAACAGCTGACGGTCCAGGTCGCAGAA
287 - 308   K K K K K K K S E E K K N N Q L T V Q V A E
925 - 990 GACTCCTTACCAGACATCCATGAGATATCGTCCAATTTCCCTAAGTCACGAAAGACGAGTGGAGA
309 - 330   D S F T D I H E I S S N S P K S R K D E W R
991 - 1056 GAAGACAAGAACAGCCAGACCCCGTAGTGTCAATGACTGTGACGCCAGGAAAGAGGGCGCTACAG
331 - 352   E D K N S Q T P L V S M T V T P G K R A L Q
1057 - 1122 GTGAGCCAGTTTATCGAAGAGAAGCAGAGGATATCACTGTCAAAGGAGAGCGCGCGCCCGGACC
353 - 374   V S Q F I E E K Q R I S L S K E R R A A R T
1123 - 1188 CTAGGCATCATATGGGGTCTTTGTAGTCTGCTGGCTCCCCTTCTTCTCATGTACGTGCTCCTC
375 - 396   L G I I M G V F V V C W L P F F L M Y V V L
1189 - 1254 CCGTTCTGCCCCACCTGCTGCCATCCGACAAGTTGGTCAACTTCATCACTTGGCTGGGCTACATC
397 - 418   P F C P T C C P S D K L V N F I T W L G Y I
1255 - 1320 AACTCCGCTCTCAATCAATCATATACACCATTTTCAATCTCGATTTCAGGAGAGCATTTAAGAAG
419 - 440   N S A L N P I I Y T I E N L D F R R A F K K
1321 - 1347 CTCCTTCATATCAAGTCTCAGACGTGA
441 - 448   L L H I K S Q T *

```

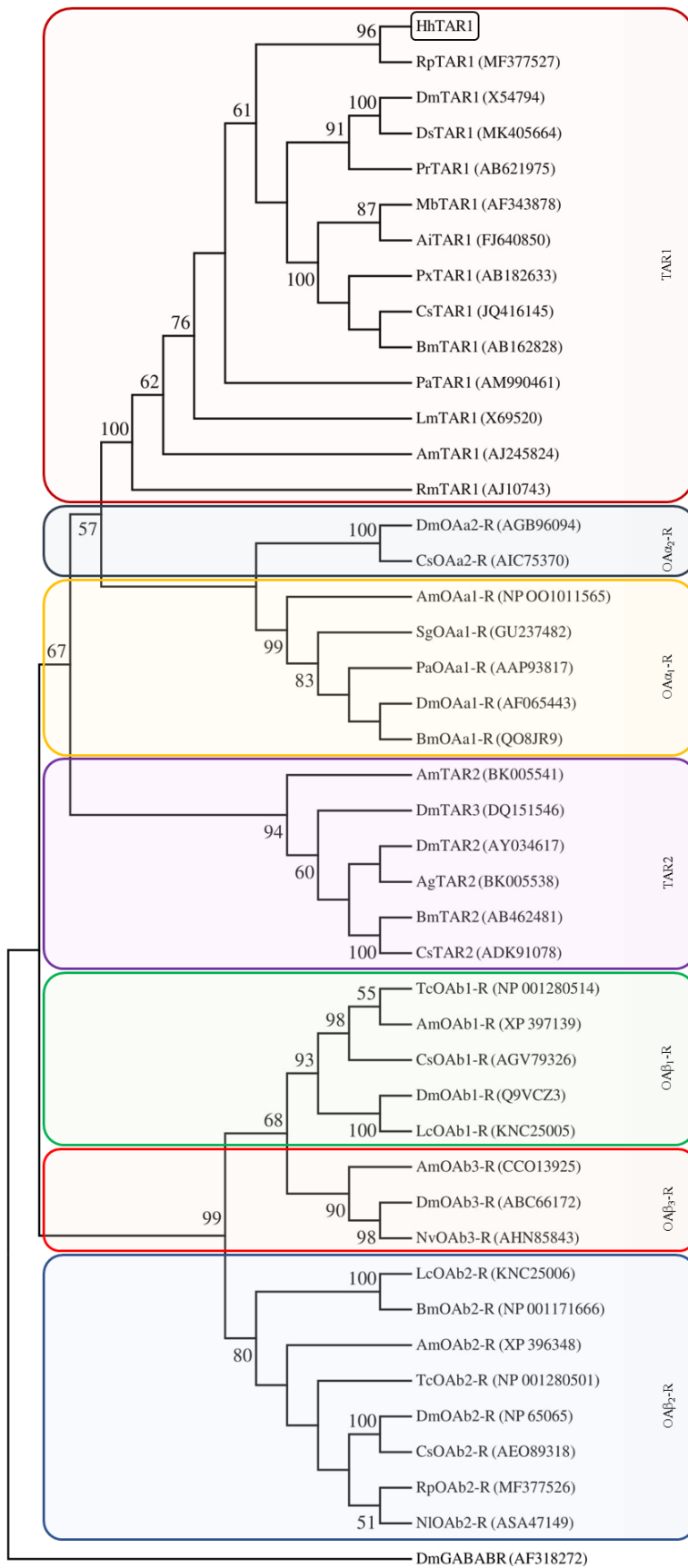
842

843 **Supplementary figure 1 (S1).** Nucleotide sequence of the TAR1 open reading frame cloned from *Halyomorpha halys*  
844 and deduced amino acid sequence. Prediction of the transmembrane segments (underlined and numbered from I to VII)  
845 was obtained with TMHMM v. 2.0 software. After the third transmembrane domain there is the DRY motif (highlighted  
846 with a box). Potential sites for N-linked glycosylation (predicted with NetNGlyc 1.0 server) are shown with a ● and  
847 potential sites for PKA or PKC phosphorylation (predicted with NetPhos 3.1 server) are shown with a † and a ‡  
848 respectively.

849

850

851 **Supplementary Figure 2 (S2)**



853

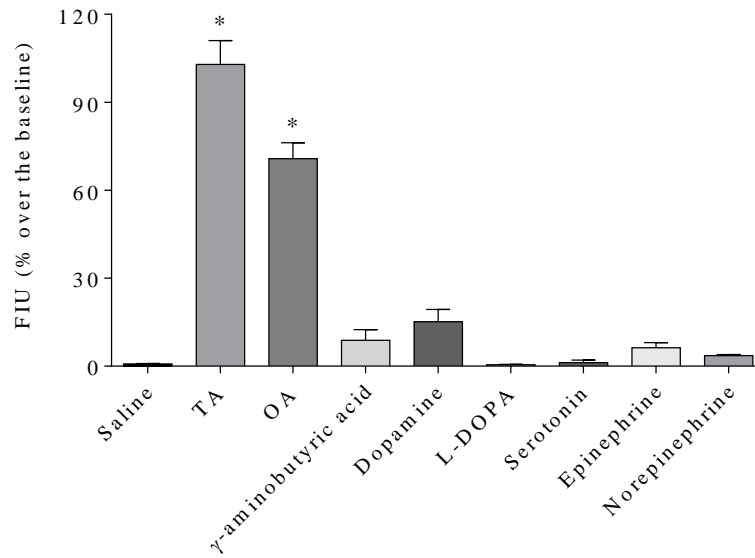
854 **Supplementary figure 2 (S2).** Phylogenetic relationships of HhTAR1 and other insect amine receptors resulting from  
855 neighbour joining analysis, using MEGA7. The values shown at the nodes of the branches are the percentage bootstrap  
856 support (1000 replications) for each branch. Alignment was performed using the amino acid sequences found in GenBank  
857 (accession number are indicated). *Drosophila melanogaster* GABA-B receptor (DmGABABR) was chosen as outgroup.  
858 Dm, *Drosophila melanogaster*; Ds, *Drosophila suzukii*; Pr, *Phormia regina*; Hh, *Halyomorpha halys*; Rp, *Rhodnius*  
859 *prolixus*; Px, *Papilio xuthus*; Cs, *Chilo suppressalis*; Bm, *Bombyx mori*; Ai, *Agnotis ipsilon*; Mb, *Mamestra brassicae*;  
860 Pa, *Periplaneta americana*; Lm, *Locusta migratoria*; Am, *Apis mellifera*; Rm, *Rhipicephalus microplus*; Sg, *Schistocerca*  
861 *gregaria*; Ag, *Anopheles gambiae*; Tc, *Tribolium castaneum*; Nv, *Nilaparvata lugens*; Lc, *Lucilia cuprina*; Nl,  
862 *Nilaparvata lugens*.

863

864

865

866 **Supplementary Figure 3 (S3)**



867  
868 **Supplementary figure 3 (S3).** Effect of biogenic amines and  $\gamma$ -aminobutyric acid on the intracellular calcium release in  
869 HEK 293 stably expressing HhTAR1. All compounds were tested at  $10^{-4}$  M. Data represent means  $\pm$  SEM of three separate  
870 experiments performed in duplicate. \*  $p < 0.001$  vs saline according to one-way ANOVA followed by Dunnett's multiple  
871 comparison test.

872

873

874 **Supplementary Figure 4 (S4)**



875

876 **Supplementary figure 4 (S4).** Image of dsRNA topically delivered on a *H. halys* 2<sup>nd</sup> instar nymph. The 2<sup>nd</sup> instar nymphs  
877 were collected 3 days post-ecdysis and placed on double-sided adhesive tape to avoid movements. One µl of the dsRNA  
878 solution was placed on the dorsal side of the abdomen. When the dsRNA solution was completely absorbed, the nymphs  
879 were put back in the nursery cage.